

## VIBRATION ISOLATION OF A ROTATING MACHINE



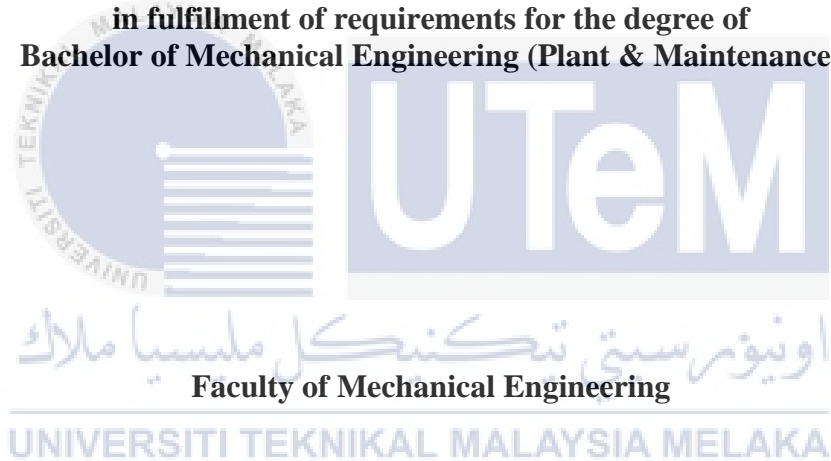
MUHAMMAD FITRI BIN RAZALI

UNIVERSITI TEKNIKAL MALAYSIA MELAKA

# **VIBRATION ISOLATION OF A ROTATING MOTOR**

**MUHAMMAD FITRI BIN RAZALI**

**A report submitted  
in fulfillment of requirements for the degree of  
Bachelor of Mechanical Engineering (Plant & Maintenance)**



**UNIVERSITI TEKNIKAL MALAYSIA Melaka**

**2017**

## DECLARATION

I declare that this project report entitled “Vibration Isolation of A Rotating Machine” is the result of my own work except as cited in the references

Signature : .....

Name : .....

Date : .....



اونيورسيتي تيكنيكل مليسيا ملاك

UNIVERSITI TEKNIKAL MALAYSIA MELAKA

## APPROVAL

I hereby declare that I have read this project report and in my option this report is sufficient in term of scope and quality for the award of the degree of Bachelor of Mechanical Engineering (Plant & Maintenance).

Signature	:	.....
Supervisor's Name	:	.....
Date	:	.....



اونيورسيتي تيكنيكل مليسيا ملاك

---

UNIVERSITI TEKNIKAL MALAYSIA MELAKA

## **DEDICATION**

To my beloved Ibu, Boboy, Fazli, Ijoy and Faiz

Thank you for your love, care and support.



## ABSTRACT

Vibration isolator is widely used in industrial fields as vibration insulation in rotating machinery. It helps to isolate the vibration of the motor from spreading to other places. Many studies have been conducted on vibration isolators. Most of the research is isolating the vibration signals in one direction either vertical direction or horizontal direction only. The study in multi-direction vibration isolation is still lacking. The purpose of this project is to study the characteristic of vibration isolator. In addition, to investigate the performance of vibration isolator and its operating deflection shape (ODS). There are a number of experiments were conducted to compare the transmissibility of two different types of vibration isolator. An experiment was conducted by using a frame; a rotating motor and some attachment of unbalance mass of the rotor. First, the experiment begun to measure the transmissibility at the frame and motor only, Then continued to frame, motor and rotor only. Next, it was continued to frame, motor, rotor and addition of unbalance mass. The present of unbalance mass actually is to produce vibrations in the system. Then, two types of vibration isolator are installed between the motor and the frame and the performance of both vibration isolator was tested. The movement of operating deflection shape (ODS) while studying the two types of vibration isolator was viewed and compared. The ODS was taken when the system is in resonance state. So that, the performance of both vibration isolator can be visualised either it is performed in a single direction or multi direction. Based on the experiment, it shows that both vibration isolator was isolated the vibration well. Besides, it shows that multi-direction type of vibration isolator isolate better than the single direction type of vibration isolator. It was proven in the both experiments either in the transmissibility performance or ODS. The ability of multi-directional vibration isolation can help reduce vibration from spreading to other places. Vibration generated from the defect machine should be isolated so that the vibrations do not cause damage.

## ABSTRAK

Penebat getaran banyak digunakan di dalam bidang perindustrian sebagai penebat getaran pada mesin yang berputar. Ianya membantu untuk menyekat getaran motor daripada merebak ke tempat lain. Banyak kajian mengenai penebat getaran telah dijalankan. Kebanyakan kajian adalah menebat getaran dalam satu arah sama ada arah mencancang ataupun arah mengufuk sahaja. Kajian terhadap penebatan getaran dari pelbagai arah masih kurang. Tujuan projek ini dijalankan adalah untuk mengkaji sifat penebat getaran. Selain itu, untuk menyiasat pelaksanaan penebat getaran dan menggambarkan kendalian bentuk pesongan tersebut. Terdapat beberapa eksperimen telah dijalankan untuk membandingkan tahap kebolehpindahan dua jenis penebat getaran yang berbeza. Eksperimen dijalankan dengan menggunakan rangka besi, motor yang berputar dan terdapat alat tambahan tidak seimbang yang diletakkan pada rotor tersebut. Pertama, eksperimen mula mengukur kebolehpindahan pada bingkai dan motor sahaja, Kemudian diteruskan bingkai, motor dan pemutar sahaja. Seterusnya, ia diteruskan dengan bingkai, motor, rotor dan penambahan massa tidak seimbang. Kehadiran massa ketidakseimbangan sebenarnya adalah untuk menghasilkan getaran dalam sistem. Seterusnya, dua jenis penebat getaran tersebut telah dipasang di antara motor dan rangka besi tersebut. Pergerakan kendalian bentuk pesongan semasa mengkaji kedua-dua jenis penebat getaran juga dapat dilihat dan dibandingkan. ODS telah diambil apabila sistem berada dalam keadaan resonans. Supaya, prestasi kedua-dua pengasing getaran boleh dilihat sama ada ia dilakukan dalam satu arah atau arah multi. Berdasarkan eksperimen, ia menunjukkan bahawa kedua-dua penebat getaran telah menebat getaran dengan baik. Selain itu, ia menunjukkan bahawa jenis penebat getaran multi-arah menebat getaran lebih baik daripada jenis satu arah penebat getaran. Ia telah terbukti dalam kedua-dua eksperimen sama ada dalam prestasi kebolehpindahan atau ODS. Kebolehan Penebatan getaran dari pelbagai arah dapat membantu mengurangkan getaran daripada merebak ke tempat lain. Getaran yang terhasil dari pada mesin yang rosak hendaklah di tebat dengan sebaik-baiknya supaya getaran tersebut tidak mengakibatkan kerosakan.

## **ACKNOWLEDGEMENT**

Final Year Project (FYP) was an amazing experience and a great chance for learning and professional development. Therefore, I felt grateful and such a lucky individual as I was given an opportunity to be a part of it. I am also excited about having a chance to meet so many wonderful people and professionals who guided me while completing this project.

First and foremost, I would like to express my deepest gratitude to ALLAH for giving me strength to complete this final year project successfully at a given period. I would also like to express my deepest gratitude and special thanks to the President of JK-PSM, Associate Professor Dr Azma Putra who in spite of being extraordinarily busy with his duties, took time out to hear, guide and keep students on the correct path and allowing us to carry out our final year project at given time duration.

Then, it is my radiant sentiment to place on record my best regards, deepest sense of gratitude to my supervisor, Associate Professor Dr Roszaidi bin Ramlan for his careful and precious guidance which were extremely valuable for my study both theoretically and practically.

I would also like to convey my sincere gratitude to my project examiners Dr Rainah binti Ismail and Associate Professor Dr. Azma Putra. Without their kind direction and proper guidance this final year project would have been little success. Not to forget to my parent, seniors and friends for keep supporting and encouraged me in completing this final year project.

I perceive as this opportunity as a big milestone in my future career development. I will strive to use gained skills and knowledge in the best possible way, and I will continue to work on their improvement, in order to attain desired future career objectives. Thank you.



---

## TABLE OF CONTENT

	PAGE
<b>DECLARATION</b>	
<b>DEDICATION</b>	
<b>ABSTRACT</b>	i
<b>ABSTRAK</b>	ii
<b>ACKNOWLEDGMENTS</b>	iii
<b>TABLE OF CONTENTS</b>	iv
<b>LIST OF FIGURES</b>	vi
<b>LIST OF APPENDICES</b>	ix
<b>LIST OF ABBREVIATIONS</b>	x
<b>LIST OF SYMBOLS</b>	xi
<b>CHAPTER</b>	
<b>1. INTRODUCTION</b>	
1.1 Background	1
1.2 Problem Statement	2
1.3 Objective	3
1.4 Scope Of Project	4
1.5 General Methodology	5
<b>2. LITERATURE REVIEW</b>	
2.1 Characterizations of Vibration Isolator	6
2.2 Transmissibility	9
2.3 Operating Deflection Shape (ODS)	14
2.4 Measurement Required For ODS	15
2.5 Rotating Machinery	18
<b>3. METHODOLOGY</b>	
3.1 Introduction	20
3.2 Analytical Study of Characteristic of Vibration Isolator	21
3.2.1 The Effect of Stiffness on Transmissibility	22

3.2.2	The Effect of Damping on Transmissibility	23
3.3	Experimental Setup	25
3.4	Measurement of Tthe Performance of Vibration Isolator	33
3.5	Operating Deflection Shape (ODS) Setup	35
<b>4.</b>	<b>RESULT AND DISCUSSION</b>	
4.1	Introduction	37
4.2	Transmissibility	37
4.3	Operating Deflection Shape (ODS)	43
<b>5.</b>	<b>CONCLUSION AND RECOMMENDATIONS</b>	53
	<b>REFERENCE</b>	57
	<b>APPENDICES</b>	60



## LIST OF FIGURES

FIGURE	TITLE	PAGE
1.1	Various types of vibration isolator	1
1.2	General methodology	5
2.1	Cooling tower	7
2.2	Vibration isolation systems	8
2.3.	Isolators subjected to force excitation	10
2.4	Isolators subjected to base excitation	10
2.5	Single degree of freedom of mass and isolator model	11
2.6	Transmissibility against non-dimensional frequency.	13
2.7	The real components of the ODS FRF's.	16
2.8	The first four ODS	17
2.9	Shaft disk model	19
3.1	Flow chart of the project.	20
3.2	Mass-Spring-damping system.	21
3.3	Free vibration without damping.	22
3.4	Simple harmonic motion of the mass-spring system.	22
3.5	Mass spring damping model.	23
3.6	General setup of the experiment.	26

3.7	Rotor design	27
3.8	Vibration isolator A.	28
3.9	Vibration isolator B.	28
3.10	Electric Motor.	30
3.11	Frame and dimension (Top and Side View)	31
3.12	Frame and dimension.	31
3.13	Slotted mass and dimension	32
3.14	General experimental setup for ODS.	35
4.1	Transmissibility against speed for motor only	38
4.2	Transmissibility against speed for motor and rotor only	39
4.3	Transmissibility against speed for motor, rotor and unbalance load	40
4.4	Transmissibility against speed for existence of Vibration Isolator A	41
4.5	Transmissibility against speed for existence of Vibration Isolator B	42
4.6	Properties of the measurement for Vibration Isolator A and B	43
4.7	Front view maximum positive animation images for Vibration Isolator A	44
4.8	Front view maximum negative animation images for Vibration Isolator A	45
4.9	Front view maximum positive animation images for Vibration Isolator B	45
4.10	Front view maximum negative animation images for Vibration Isolator B	46
4.11	Side view maximum positive animation images for Vibration Isolator	47
4.12	Side view maximum negative animation images for Vibration	47

	Isolator A	
4.13	Side view maximum positive animation images for Vibration Isolator B	48
4.14	Side view maximum negative animation images for Vibration Isolator B	48
4.15	Top view maximum positive animation images for Vibration Isolator A	50
4.16	Top view maximum negative animation images for Vibration Isolator A	50
4.17	Top view maximum positive animation images for Vibration Isolator B	51
4.18	Top view maximum negative animation images for Vibration Isolator B	51



## LIST OF APPENDICES

APPENDIX	TITLE	PAGE
Appendix A	Gantt chart	61
Appendix B	Data analysis for transmissibility	62
Appendix C	Operating Deflection Shape Experiment	65



## LIST OF ABBREVIATIONS

T	Transmissibility
ODS	Operating Deflection Shape



## LIST OF SYMBOL

$c$	=	Damping coefficient
$\xi$	=	Damping ratio
$F_e$	=	Excitation force
$F_t$	=	Force transmitted
$i$	=	$\sqrt{-1}$
$m$	=	Mass
$k$	=	Spring stiffness
$\omega$	=	Operating frequency
$\omega_n$	=	Natural frequency
$T_f$	=	Transmissibility
$x$	=	Displacement
$\dot{x}$	=	First derivatives of $x$
$\ddot{x}$	=	Second derivatives of $x$





## CHAPTER 1

### INTRODUCTION

#### 1.1 BACKGROUND



Figure 1.1 Various types of vibration isolators.

Nowadays, there are many types of vibration isolator as shown in Figure 1.1 that has been used and required in various industrial sectors or everyday objects in order to reduce the vibration transmission, such as in pumps, motors, HVAC systems, isolation of civil engineering structures, base isolation, sensitive laboratory equipment and valuable statuary. Besides, vibration isolators are also widely used in machinery as vibration insulation, which blocks the vibration waves from transfers to the floor. As the machine, continuously operating in a long period of time, under a high speed and carry heavy loads; indirectly it will cause a critically damaged. The problem is getting worse when, the vibration waves are transmitted to the other machine that stay next to the machine produced vibrations.

The vibration phenomenon might be occurred due to the problems inside the operating machine. The unbalance and misalignment of existing components of the machines might be one of the several reasons that lead to a high vibration of the machine component and can cause the machine breakdown. Thus, the vibration waves produced from the machine is not properly isolated. It will transmit to the floor. From the floor, it will transmit to the machines that stay next to the problem machine. In this case, it produces another problem to the machine next to it. As the result, it might affect the performance of the machine to operate. The operation of the machine will be decreased and could be a danger for user to run the machine. Thus, the maintenance cost would be higher if there is a critical damage or broken part of the machine component.

As the solution to this problem, vibration insulation is required to isolate the machine in order to reduce the vibration waves from transmit to another part. The present of vibration isolator on the machine, will block or decreases the vibration waves from transmitting to others part. As a result, it will produce another problem to the machine that stays next to it. Thus, this vibration problem will contribute to the decreasing performance of the machine. The machine could be dangerous to the user while running the machine and cause the machinery breakdown. As we know, currently the maintenance cost would be high when critical damage or broken part of the machine component. To avoid this problem to become worse, we need to isolate the vibrations that produce from the defect machine.

## 1.2 PROBLEM STATEMENT

Nowadays, there are need to isolate the vibration waves that are produced from the defect machine. But, currently there are so many vibration isolators that isolate the vertical vibration of the machine were produced. The problem occurs when, current vibration isolators does not work in multi-degree of freedom which is only work in one direction and unable to work more than one direction. We know that, when the machine is defected, it will vibrate not in single degree of freedom (one direction). The machine will vibrate in multi-degree of freedom various directions which are mostly in vertical and lateral direction. Currently, most of the isolators produced are effective in one direction, such as vertical vibration. Thus, only few numbers of isolator are effective in overcoming the lateral direction. The problem occurs when the lateral vibration is damaging as much as the vertical direction as well. So that, there are need to take care of this vibration problem.

## 1.3 OBJECTIVE

The objectives of this project are as follows:

1. To study the characteristic of vibration isolator.
2. To measure the performance of vibration isolator using measured data.
3. To visualize the effect of vibration isolator on the motor vibration Operating Deflection State (ODS)

## 1.4 SCOPE OF PROJECT

The scopes of this project are:

1. Obtain the characteristic of vibration isolator by conducting analytical studies.
2. Do the experimental work in order to measure the performance of two types of vibration isolators of input and output as well as to measure data by using accelerometer sensor.
3. Obtain the motor vibration ODS (Operating Deflection State) pattern and visualize the effect of two different types of vibration isolator by using VibShape Software.



## 1.5 GENERAL METHODOLOGY

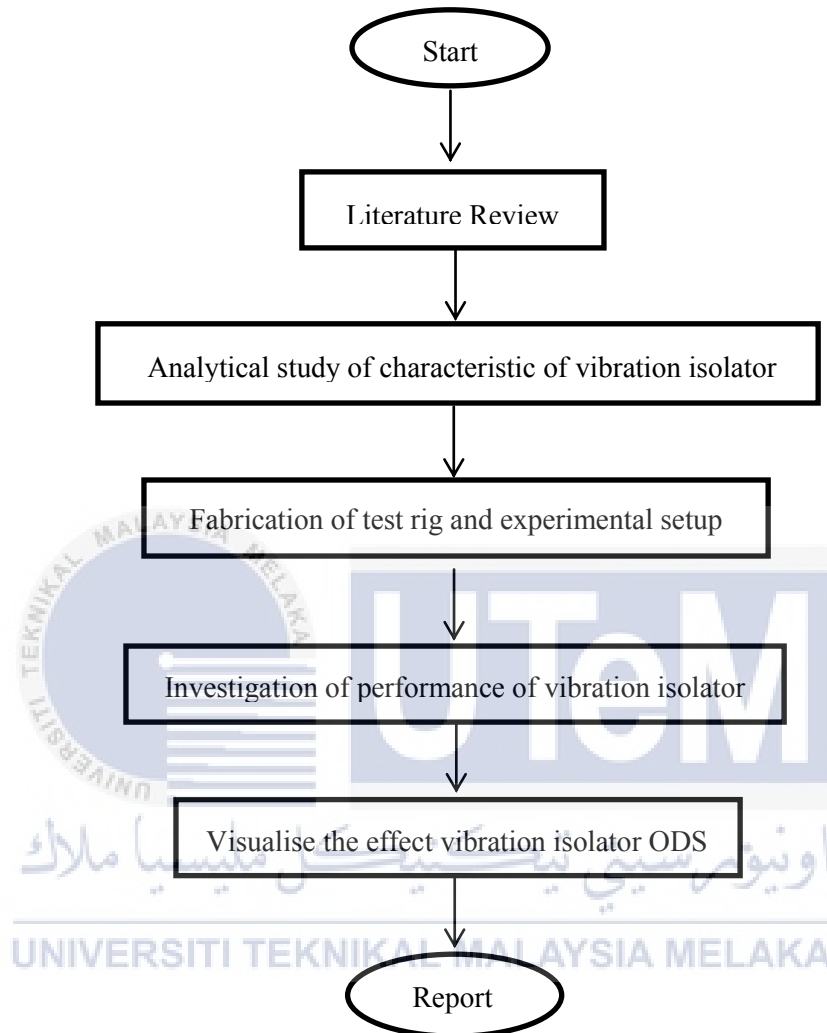


Figure 1.2 General Methodology

## CHAPTER 2

### LITERATURE REVIEW

#### 2.1 Characterizations of Vibration Isolator

Vibration isolators are used in many applications to minimize the transfer of vibrations from machines to foundations. This is always the case in domestic appliances, a typical example being refrigerators where vibration isolators are used to minimize the structural borne noise due to the vibrations of the compressor. According to Levent and Sanliturk (2003) for this particular case compressor grommets are the vibration isolators which are used to minimize the transfer of vibrations from compressor to refrigerator body. However, the optimization of vibration isolators is a difficult process mainly due to inherent dependency of the properties of viscoelastic materials to many factors, including temperature, frequency and strain.

In addition, Naibiou (2011) stated that, vibration isolator is one of the vibration suppression methods. There are two kinds of vibration isolation which are to isolate a vibration source from its support and to isolate a base excitation from a device (Coppola, 2010). Furthermore, a simplest vibration isolator consists of a spring and a damper arranged in parallel. The spring plays a dual role which is to support the weight of the device and to isolate the base motion. Meanwhile, for a linear spring isolator, vibration isolation occurs when the natural frequency of the isolator system is smaller than the frequency of the base motion or exciting frequency. According to Carrella et al. (2008)

stated that to increase the isolation region, the stiffness of the isolator spring should be made as low as possible. However, lowering the isolator's stiffness results in a large static deflection that is undesirable. To overcome this problem, a high-static-low-dynamic stiffness (HSLDS) spring can be used. The HSLDS isolator is capable of supporting a large static load while possessing a low natural frequency.



Figure 2.1 Cooling Tower

Lamancusa (2002) stated that, by referring to the Figure 2.1 it shows a common example the vibration sources with a large reciprocating air conditioning compressor weighing 20,000 pounds, mounted on a roof. The loud noise levels at multiples of the compressor rotational frequency, predominantly 60 and 120 Hz, were measured in the rooms directly below the compressor.

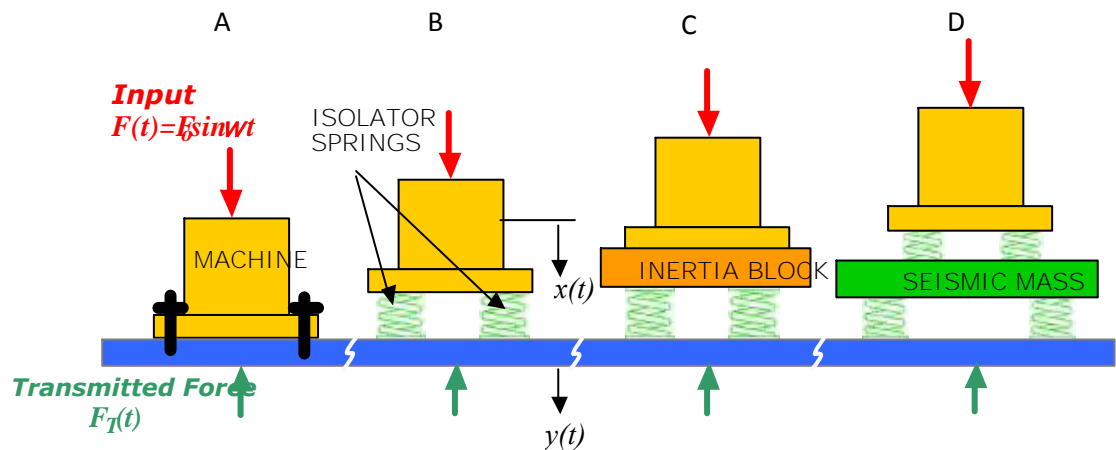


Figure 2.2 Vibration isolation systems

Based on Figure 2.2, there are four systems which are

- A) Machine bolted to a rigid foundation
- B) Supported on isolation springs, rigid foundation
- C) Machine attached to an inertia block
- D) Supported on isolation springs, non-rigid foundation (such as a floor); or a machine of isolation springs, seismic mass and second level of isolator springs

According to Figure 2.2, B is the force transmitted to the floor is equal to the force generated in the machine. The transmitted force can be decreased by adding a suspension and damping elements are known as vibration isolators. Based on Figure 2.2, C by adding an inertia block, a large mass which is a block of cast concrete, will directly attach to the machine. According to Figure 2.2, D another option is to add an additional level of mass or known as a seismic mass, again a block of cast concrete and suspension (Lamancusa, 2002).



## 2.2 Transmissibility

According to Schwarz and Richardson (2004) stated that a transmissibility measurement is similar to a Frequency Response Function (FRF) measurement, but uses roving and reference response signals instead of a force and a response signal pair. Other than that, the transmissibility is defined as the Fourier spectrum of the roving response divided by the Fourier spectrum of the reference response. It is actually computed by dividing the cross spectrum between the roving and reference responses by the auto spectrum of the reference response.

In addition, Potter (2003) stated that, as with FRFs, a set of Transmissibility's contains both magnitude and phase at each frequency, so ODS's obtained from a set of Transmissibility's will also contain correct magnitude and phase information. The units of the operating deflection shapes are response units per unit of response at the reference DOF. According to Ravindra and Mallik (as cited in Zhenlong, Xingjian and Li, 2012) analyses the vibration isolators having nonlinearity in both stiffness and damping terms under both force and base excitations. The transmissibility was obtained by the method of harmonic balance, and the effects of various types of damping to the transmissibility were also studied.

Milovanovic et al (2009) studied that the vibration isolators with linear and cubic nonlinearities in stiffness and damping terms under based excitation. The influence of the nonlinear parameters on the displacement transmissibility was studied, and they presented that the absolute displacement transmissibility of the isolator with cubic damping tends to unity as  $O-N$ , which corresponds to a rigidly connected system. Besides, by using the concept of Output Frequency Response (OFR) function, the analytical relationship

between the force and absolute displacement transmissibility and the nonlinear damping coefficient of the vibration isolator are derived (Jing et al. 2011).

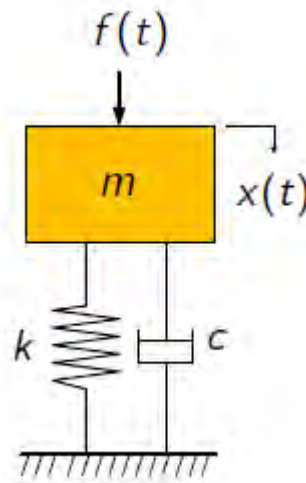


Figure 2.3 Isolators subjected to force excitation.

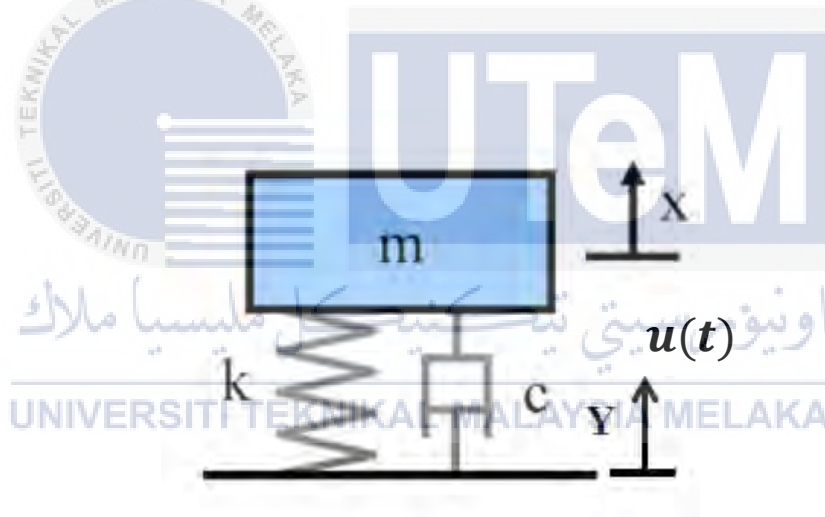


Figure 2.4 Isolators subjected to base excitation.

According to Zhenlong et al (2012) showed the example of nonlinear isolators subjected to force excitation and base excitation which have been conducted by them. The linear isolator is modelled as a parallel combination of a linear spring with stiffness,  $k$  and a linear damper,  $c$ . Both are located at between mass and base as shown in Figure 2.3 and the Eq. (2.1) is given as:

$$m\ddot{x} + c\dot{x} + kx = f(t) \quad (2.1)$$

Based on the formula above,  $c$  is the linear damping coefficient. In Figure 2.3 shows the force excitation. Eq. (2.2) shows the equation of force excitation:

$$f(t) = A \sin(\omega t) \quad (2.2)$$

Directly exerted on the mass,  $m$  with amplitude,  $A$  and frequency  $\omega$ . In Figure 2.4, the input base excitation equation is Eq. (2.3) where  $A$  is the amplitude and  $\omega$  is the excitation frequency:

:

$$u(t) = A \sin(\omega t) \quad (2.3)$$

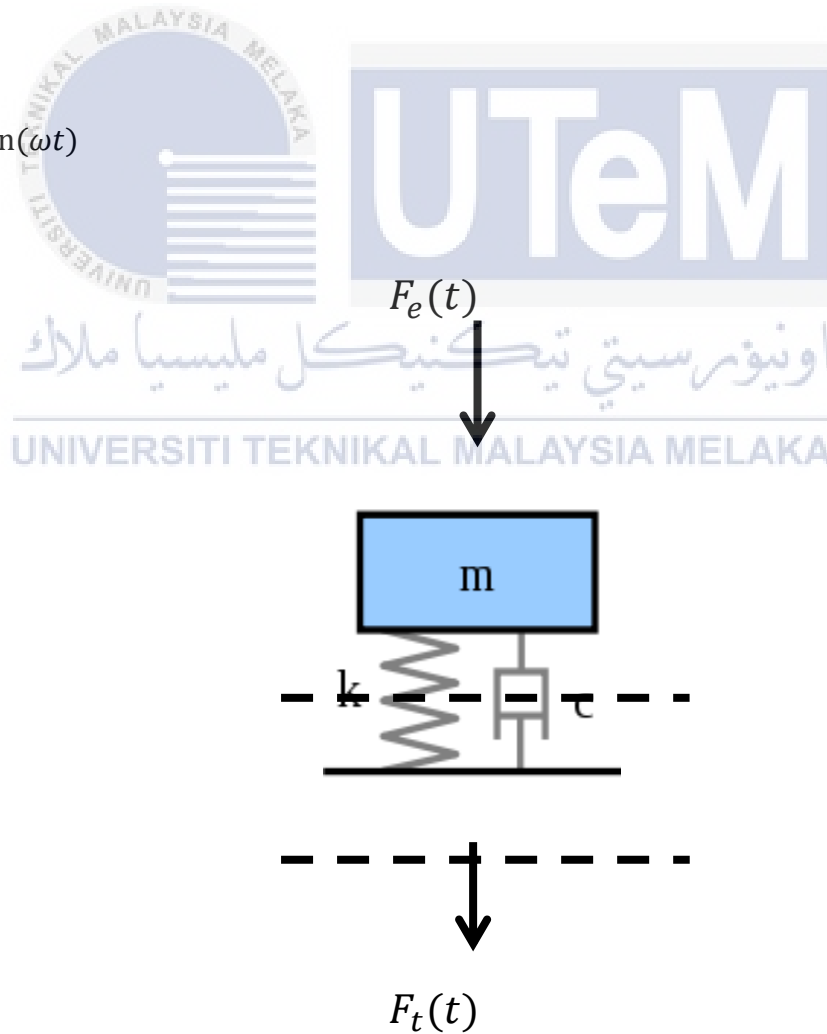


Figure 2.5 Single degree of freedom of mass and isolator model.

Consider a machine with mass  $m$  installed on a structure through an elastic support having stiffness  $k$  and damping constant  $c$ . A single degree of freedom model can be assumed as shown in Figure 2.5. The transmissibility  $T_f$  is defined as the ratio of the transmitted force,  $f_t(t)$  injected into the structure of the excitation force,  $f_e(t)$  excited by the machine. The equation of motion can be obtained by using Newton's second law as given:

$$\frac{c(t)}{dt} + kx(t) = f_e(t) \quad (2.4)$$

Assuming the force is harmonic, then  $f_e(t) = F_e e^{j\omega t}$  and  $x(t) = X e^{j\omega t}$  where  $F_e$  and  $X$  are the complex amplitudes and  $\omega$  is the excitation frequency.

$$F_e = (-\omega^2 m + j\omega c + k)X \quad (2.5)$$

Substituting this to Eq.(2.5) gives similarly for the transmitted force, one can obtain

$$F_t = (k + j\omega c)X \quad (2.6)$$

Dividing Eq. (2.6) with Eq.(2.3), the transmissibility of the model is obtained which is written as

$$T_f = \left| \frac{F_t}{F_e} \right| = \left| \frac{k + j\omega c}{k - \omega^2 m + j\omega c} \right| \quad (2.7)$$

Substituting  $\omega_n^2 = k/m$  and  $c = 2\xi\omega_n m$  into Eq. (2.8) to show the relation between transmissibility and damping ratio, natural frequency and operating frequency

$$T_f = \left| \frac{1 + j2\xi \frac{\omega}{\omega_n}}{1 - \left( \frac{\omega}{\omega_n} \right)^2 + j2\xi \frac{\omega}{\omega_n}} \right| \quad (2.8)$$

when model is being excited at its resonance, i.e at  $\omega = \omega_n$ , the transmissibility is given by

$$T_f = \frac{1}{2\xi} > 1 \quad (2.9)$$

Eq. (2.9) shows that the force received by the receiver is amplified when it is being excite near or at its natural frequency as shown in Figure 2.6. This will cause vibration to the surrounding and noise if there is no proper isolation. If this condition prolongs, it will cause damage to the machine and cause structural failure.

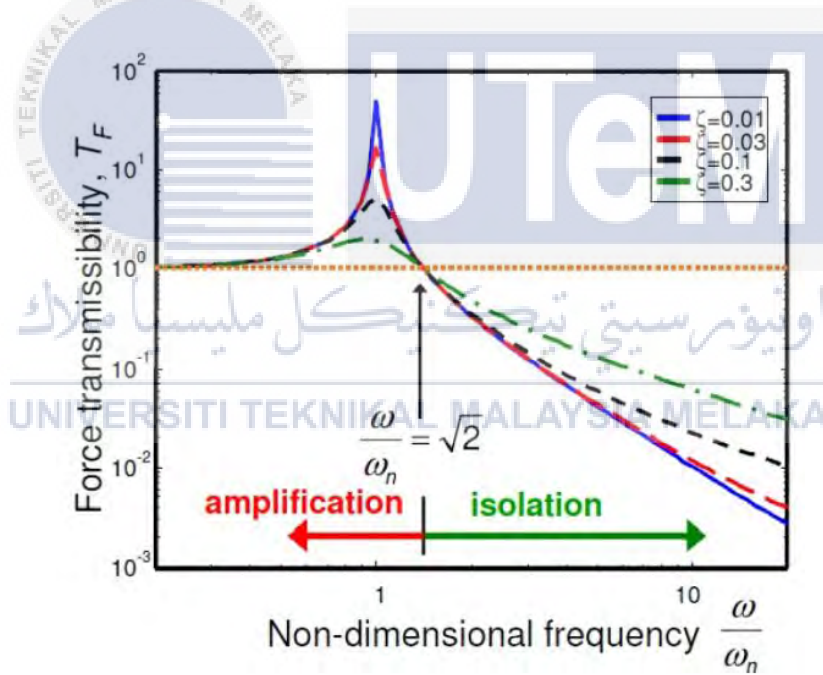


Figure 2.6 Transmissibility against non-dimensional frequency.

### 2.3 Operational Deflection Shape (ODS)

Operational Deflection Shape (ODS) has been defined as the deflection of a structure at a particular frequency. However, an ODS can be defined as any forced motion of two or more points on a structure (Schwarz and Richardson, 2004). According to Potter, (2003) specifically, the motion of two or more points defines a shape which is a shape is the motion of one-point relative to all others. In addition, motion is a vector quantity, which means that it has location and direction associated with it. This is also called a Degree of Freedom (DOF).

In depth, Kramer (2001) stated that an operating deflection shape contains the overall vibration for two or more DOFs on a machine or structure. That is, the ODS contains both forced and resonant vibration components. Other the other hand, a mode shape characterizes only the resonant vibration at two or more DOFs.

Meanwhile, resonant vibration typically amplifies the vibration response of a machine or structure far beyond the design levels for static loading. Resonant vibration is the cause of, or at least a contributing factor to many of the vibration related problems that occur in structures and operating machinery (Schwarz and Richardson, 2004). In other words, any structural vibration problem, the resonances of a structure need to be identified. A common way of doing this is to define its modes of vibration. Each mode is defined by a natural (modal) frequency, modal damping, and a mode shape.

## 2.4 Measurement Required for ODS

According to Richardson (2004) he claimed that the values of a set of time domain responses at a specific time, or the values of a set of frequency domain responses at a specific frequency. Furthermore, an ODS can be obtained from a set of measured time domain Responses of four elements which are Random, Impulsive, Sinusoidal and Ambient. All of these were important to get the accurate measurement for ODS. In addition, according to Yonghui et al. (2016) stated that to construct an ODS, the vibrations at multiple locations of the structure are measured simultaneously. Furthermore, the vibration magnitude and phase of all points define an ODS.

An ODS can be derived from a set of time domain signals acquired simultaneously or frequency domain measurements that are computed from the time domain signals (Weekes and Ewins, 2015). Other than that, Bae et al. (2011) were investigated that the ODS frequency response function (FRF) is used to construct the ODS in this study. In depth, this technique requires a fixed reference sensor in order to determine the relative phase of each measurement point. To calculate an ODS FRF, the magnitude of the cross spectrum between a sensor signal and the reference sensor signal is replaced with the auto spectrum of the sensor signal. Besides, the correct magnitude of the sensor signal and the correct phase relative to the reference signal are retained. The definition of the ODS FRF is given by the following equation:

$$H_1(f) = \frac{X(f)F^*(f)}{F(f)F^*(f)} = \frac{G_{XF}}{G_{XF}} \quad (2.10)$$

$$H_2(f) = \frac{X(f)F^*(f)}{F(f)F^*(f)} = \frac{G_{XX}}{G_{FF}} \quad (2.11)$$

In addition, according to Lynch et al. (2006) stated that the conditions of low damping and well-separated vibration modes, the ODS FRFs reach a local maximum around the resonant frequencies, which can be identified using the so-called peak picking (PP) method. Therefore, the response of the electrostatic sensor represents the transverse velocity, the real components of the ODS FRFs at the resonant frequency  $\omega_j$  are assembly as follows to yield the  $i$ -th mode shape vector  $\omega_i$ .

Moreover, to calculate the ODS FRFs of the belt, sensor S1 is selected as the reference. Figure 2.7 shows the real components of the ODS FRFs at the lower frequency band (0 to 40 Hz). As illustrated in Fig 2.7, the peaks in the amplitude spectra appear at the same frequencies in the ODS FRFs by connecting the peaks at the same frequency in Figure 2.7. The belt ODS can be constructed. Figure 2.8 depicts the ODSs corresponding to the first four vibration modes at the resonant frequencies.

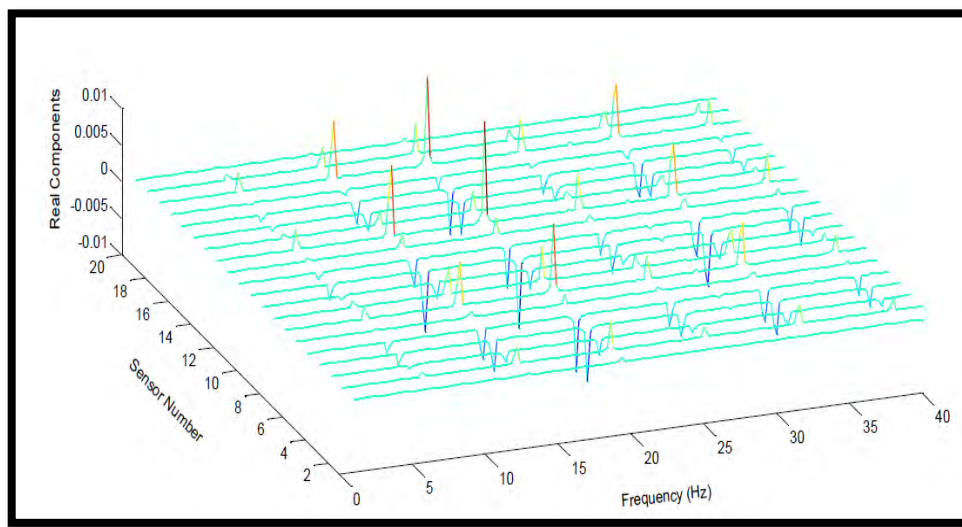


Figure 2.7 The real components of the ODS FRF's.



In addition, Lynch et al. (2006) stated that, the four ODSs exhibit similar deformation patterns, apart from the differences in magnitude. This result is different from the ODS measurement results for solid structures such as bridges, where the number of nodes increases with the mode number. Besides, the axial motion of the belt determines that the measured ODSs translate in the belt running direction, rather than staying fixed in space. The other vibration modes have similar propagating ODSs bounded by envelopes with different magnitudes.

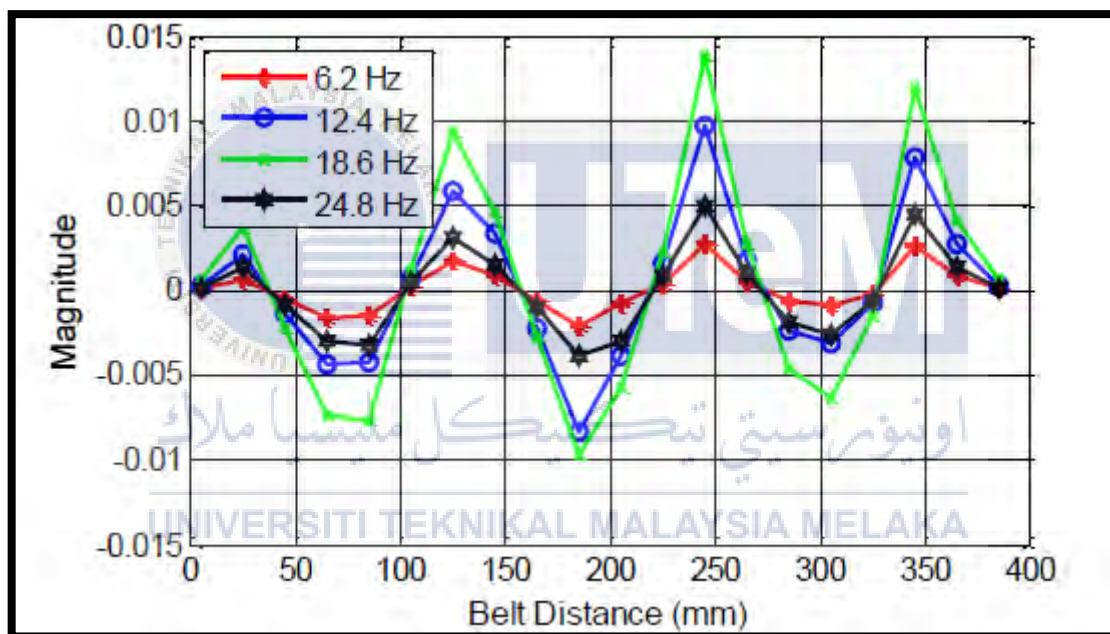


Figure 2.8 The first four ODS

## 2.5 Rotating Machinery

Modal models are widely used to describe the dynamic behavior of non-rotating structures. For modelling purposes, rotating machines can be considered as structural assemblies of rotating and non-rotating components. According to Enrique (2003), the dynamic behaviour of these assemblies is determined by the properties of their individual components and their interactions, as is the case for conventional structures formed by the assembly of purely non-rotating elements.

In the case of non-rotating structures, the damping matrix is associated with forces that are capable of reducing the mechanical energy of a system, while the stiffness matrix is associated with elastic forces, which produce a tendency of the system to move towards its static equilibrium configuration without modifying its total energy level. On the other hand, the damping and stiffness matrices of rotating machinery structures also represent the gyroscopic and circulatory forces, respectively, that arise due to rotation. The damping matrix is used to represent the damping and the gyroscopic forces, both of which have a velocity-dependent characteristic. Similarly, the stiffness matrix is used to represent elastic and circulatory forces, which have a displacement-dependent characteristic.

According to Carella et al. (2009) stated that two common types of machine are analysed using such a model, namely a rigid rotor on flexible supports, or a Jeffcott rotor consisting of a rigid disk of a flexible shaft. Besides, in both cases the machine is assumed to be symmetrical, so that the center of mass of the rotor is midway between two identical supports. In this way, out-of-balance forces applied at the center of the rotor will only excite a translational motion.

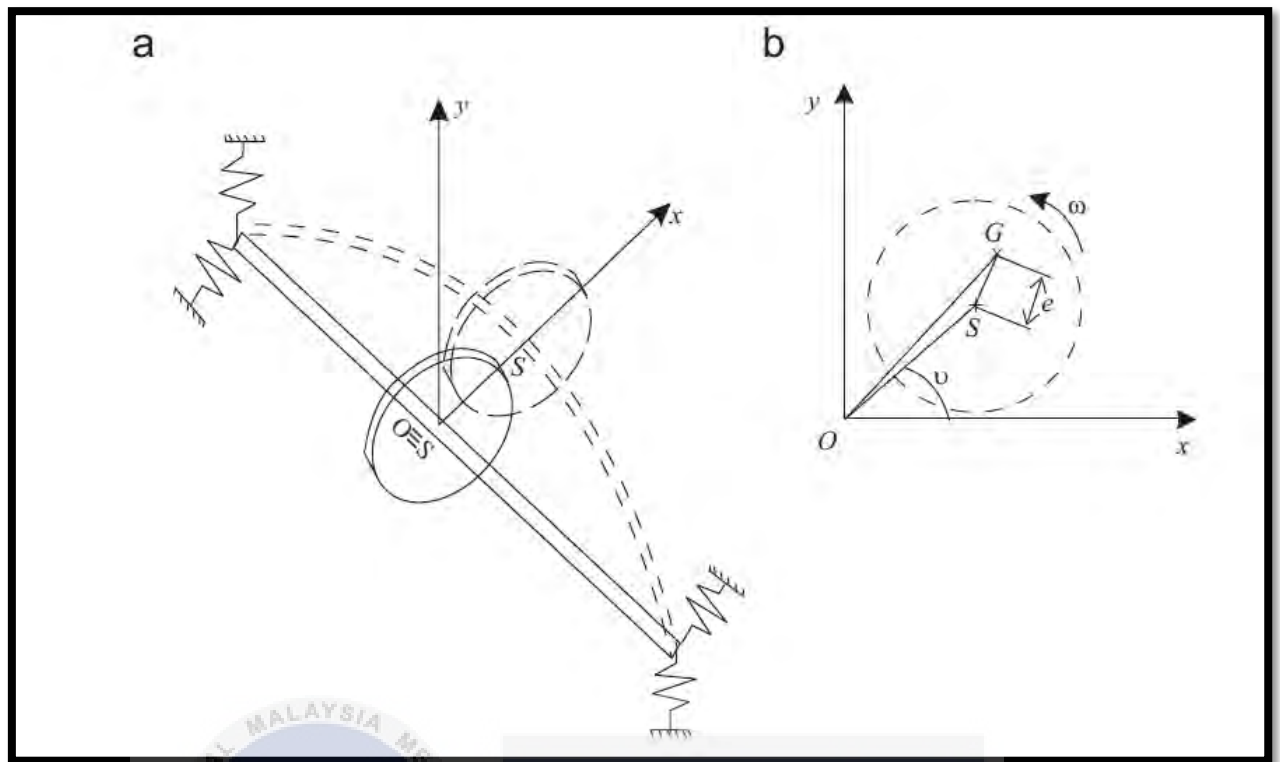


**Figure 2.9:** Shaft disk model

Based on the Figure 2.9, the picture a showed the schematic of the system in initial conditions and whirling with angular velocity, which dashed meanwhile the figure b showed the response of the disk where  $S$  is the geometric centre of the shaft and  $G$  is the center of mass of the disk and the distance  $e$  is the eccentricity. In depth, the modelled machine schematically, where the mass is concentrated in a disk located centrally on the shaft means the two degrees of freedom are the translational displacement of the disk. Both a flexible shaft and spring supports are included and since both components have negligible mass their stiffness may be combined using the formula for springs in series. Indirectly, the supports will be considered very flexible to isolate the vibration which case the rotor will essentially rigid. The shaft rotates with the angular speed  $\omega$ .

## CHAPTER 3

### METHODOLOGY

#### 3.1 Introduction

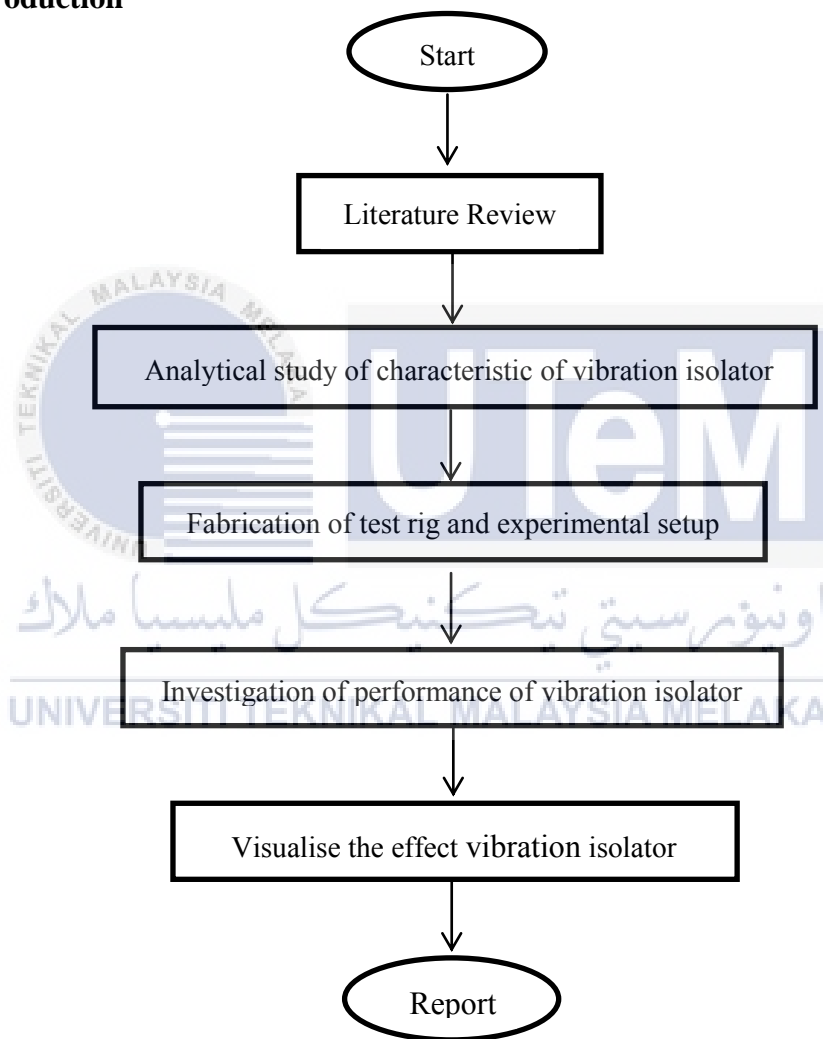


Figure 3.1 Flow chart of the project

This chapter explains the methodology used in this project, which is to isolate the vibration of a rotating motor. The flow chart of the project is shown in Figure 3.1. This project begins with the analytical study, which is to investigate the characteristic of vibration isolator. Then, the performance of the vibration isolator can be determined from the measured data of the experiment by using accelerometer sensor. Last, the effect of the vibration isolator on the rotor vibration can be visualized by Operating Deflection State (ODS) input. In this project the effect of the vibration isolator in vertical and lateral direction can be determined by two types of the different vibration isolator.

### 3.2 Analytical Study of Characteristic of Vibration Isolator

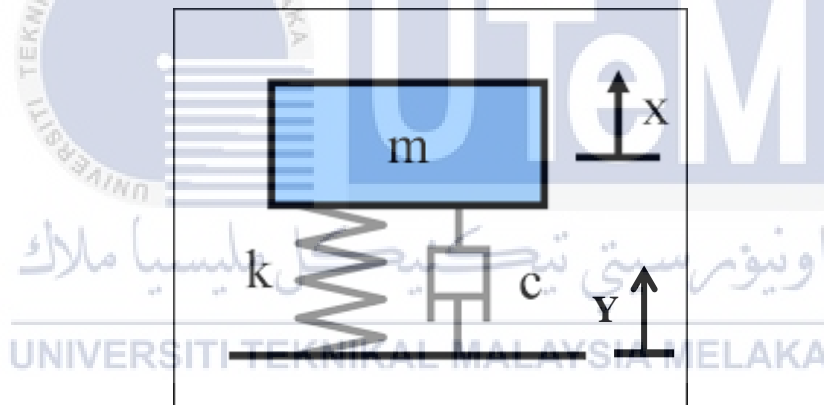


Figure 3.2 Mass-Spring-damping system.

At the beginning of this research, the study of the vibration isolator characteristics has been conducted in order to understand the fundamental concept of vibration isolator. To investigate the characteristic of the vibration isolator, the analytical study on the mass-spring-damping system has been conducted. This system is divided into two parts which are the effect of damping on the transmissibility and the effect of stiffness on the transmissibility. Figure 3.2 shows mass-spring-damping system.

### 3.2.1 The Effect of Stiffness on Transmissibility

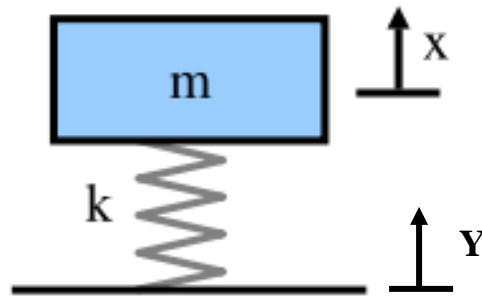


Figure 3.3 Free vibrations without damping.

For the effect of stiffness on the transmissibility, the damping of this system can be neglected. Therefore, there will be no external force applied to the mass as shown in Figure 3.3. The system is known as free vibration without damping. By assuming the spring is already compressed due to the weight of the mass, the force applied to the mass by the spring is directly proportional to the amount of the spring is stretched " $\bar{x}$ ".

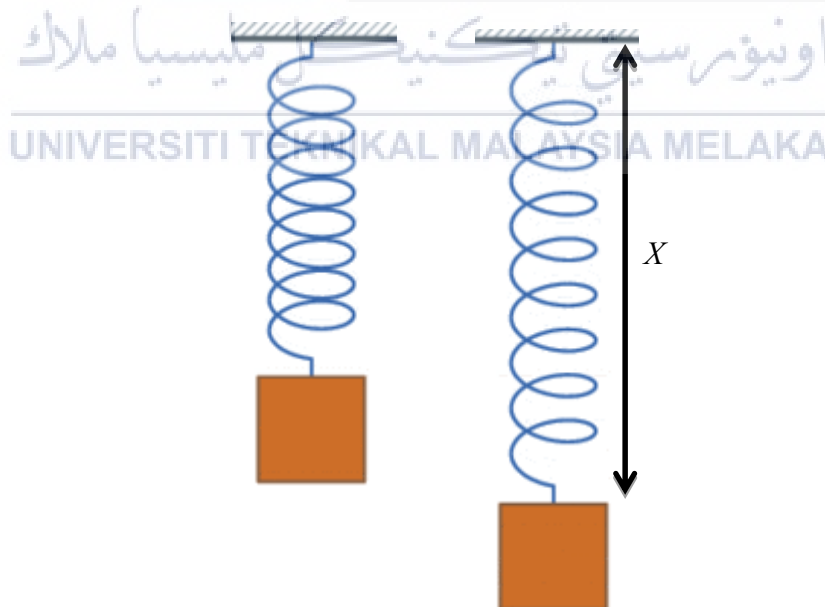


Figure 3.4 Simple harmonic motion of the mass-spring system.

The vibration motion can be explained in terms of conservation of energy. In the Figure 3.4 example the spring has been extended by a value of “ $X$ ”. Therefore, some potential energy is kept in the spring ( $\frac{1}{2}kx^2$ ). When the mass released, the process accelerates the mass and the spring tends to be un-stretched state which known as the minimum potential energy state. At this point, when the spring has reached its un-stretched state, all the potential energy that we supplied by stretching it has been changed into the kinetic energy ( $\frac{1}{2}mv^2$ ). The mass then starts to decelerate as it is now compressing the spring. In the process the kinetic energy back to its potential.

### 3.2.2 The Effect of Damping on Transmissibility

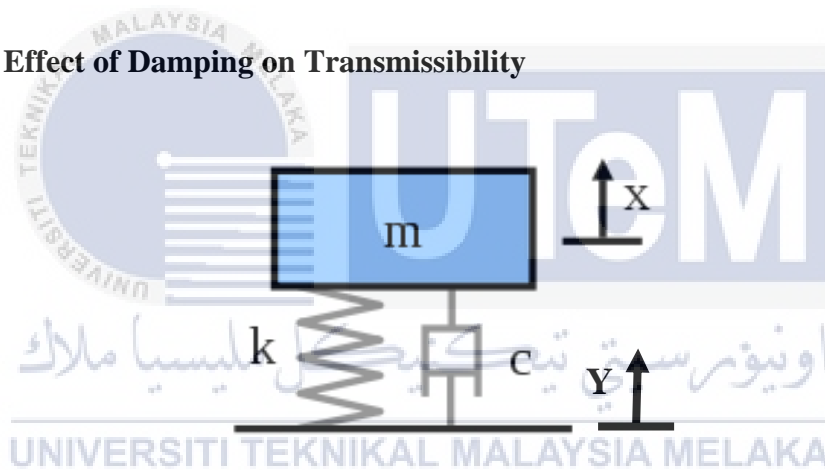


Figure 3.5 Mass spring damping model.

Figure 3.5 shows the mass spring damping model. The simple harmonic oscillator consists of a damper that added to the model. Therefore, the outputs a force that is proportional to the velocity of the mass. The “ $c$ ” is called damping coefficient. The mass spring damping model can be expressed in term of differential equation shown as Eq 3.1.

$$m\ddot{x} + c\dot{x} + kx = 0 \quad (3.1)$$

The solution of this equation depends on the amount of damping. When the damping is small, the system still vibrates, but eventually it will stop vibrating over time.

In this case it is known as underdamping. Critical damping can be reached by the system when the damping is increased just to the point where the system no longer oscillates. The damping coefficient in the mass spring damper model is shown as Eq 3.2.

$$C_c = 2\sqrt{km} \quad (3.2)$$

The amount of damping ratio can be characterized by damping ratio/damping factor. This ratio is the ratio of actual damping over the amount of damping required to reach critical damping. The formula of damping ratio of the mass spring damper model is shown as Eq 3.3.

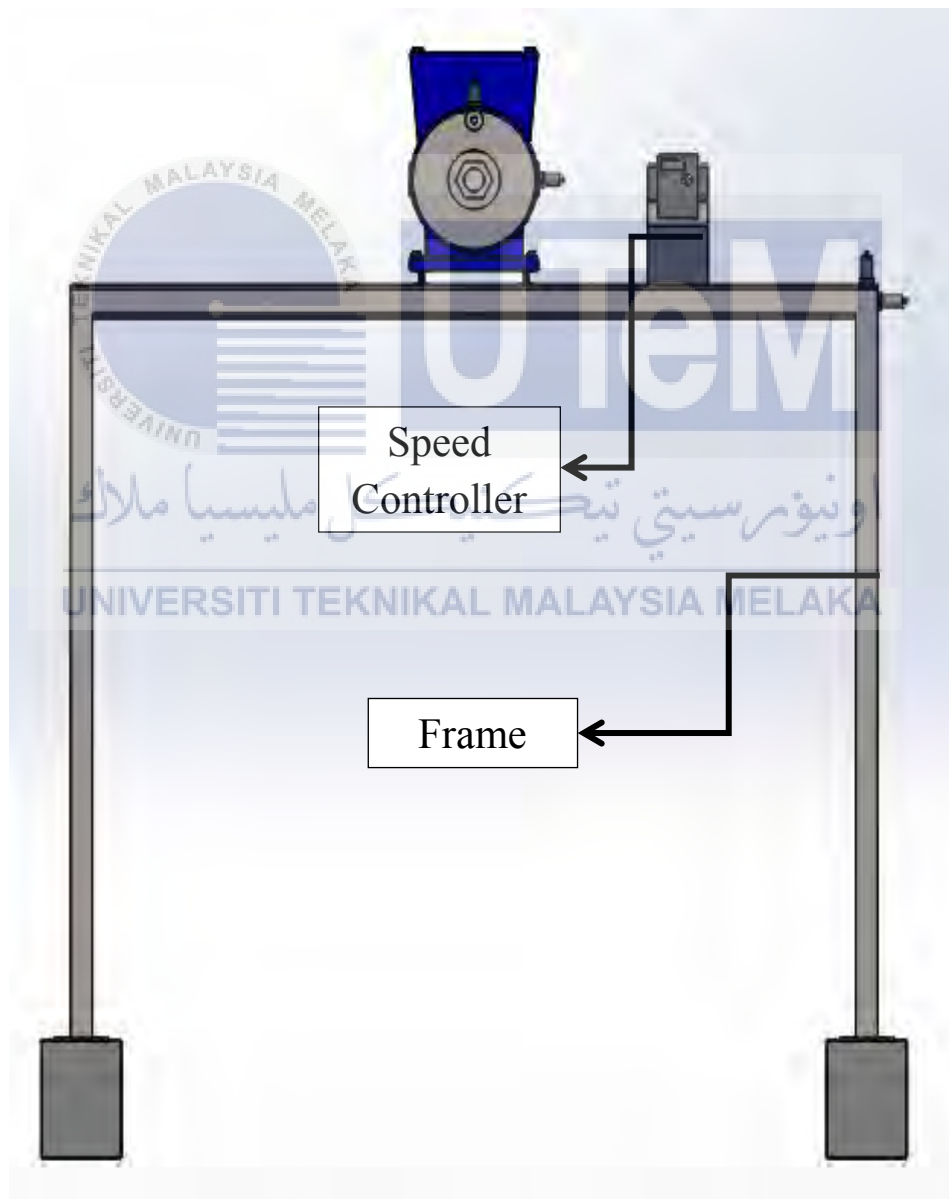
$$\xi = \frac{c}{2\sqrt{km}} \quad (3.3)$$





### 3.3 Experimental Setup

After doing the analytical study of fundamental of vibration isolator, the experiments can be conducted in order to investigate the performance of two different types of vibration isolator. The performance of two different types of vibration isolators can be measured during conducting the experiment. The purpose of this experiment is to study the performance of each vibration isolator. Figure 3.6 shows the general setup of the experiment.



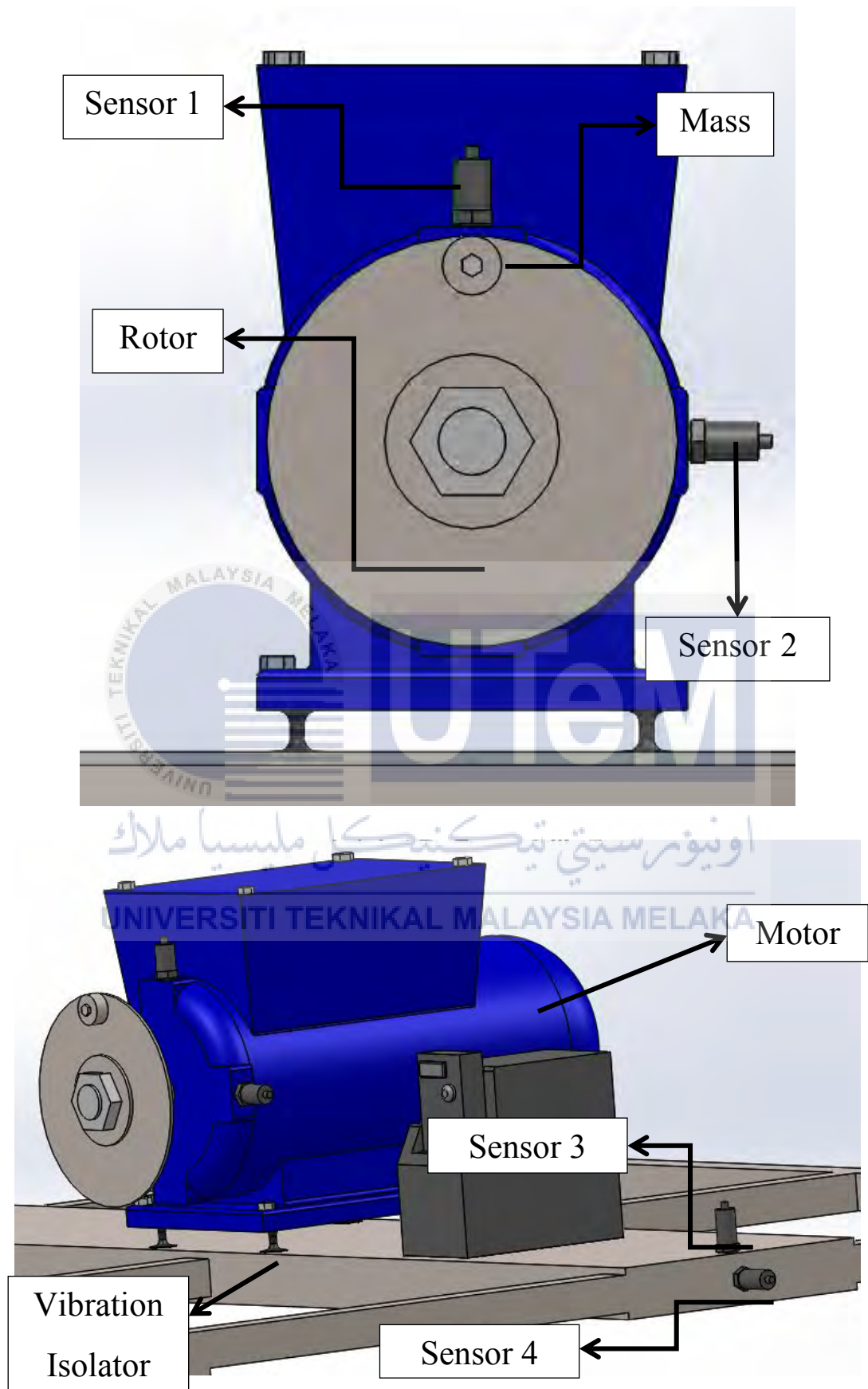


Figure 3.6 General setup of the experiment.

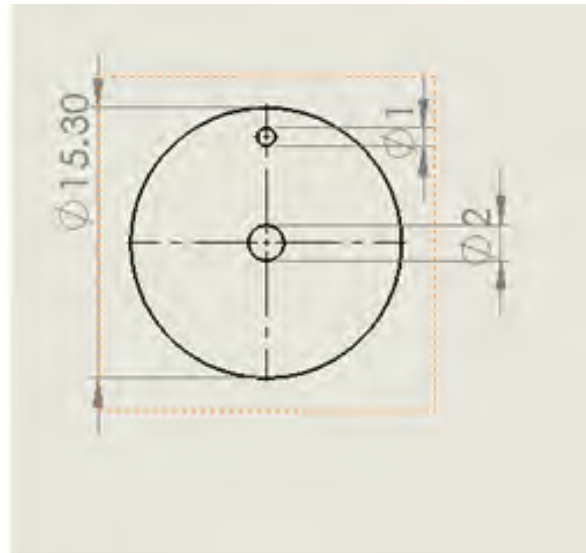


Figure 3.7 Rotor design

Figure 3.7 shows a rotor design that's being used in this experiment. The function of the rotor is to create unbalance rotation when it is attached together with motor's shaft. The slotted mass will be attached at the rotor. When the motor operates, the rotor will rotate together with the slotted mass. An unbalance rotation will produce and vibration will be occurred. The diameter of the rotor is 15.3cm. The diameter of the center hole is 2cm. The diameter of the other hole is 1.0cm. The thickness of the rotor is 0.1cm.

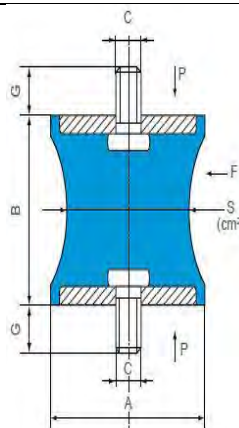
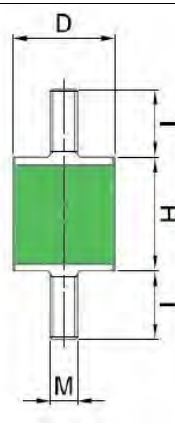


Figure 3.8 Vibration isolator A



Figure 3.9 Vibration isolator B

**Table 3.1:** Specifications for Vibration Isolator A and B

		
	Vibration Isolator A	Vibration Isolator B
Dimensions	A- 57mm B- 44mm C- M8 G- 20mm S- 5cm <sup>2</sup>	D- 25mm H- 20mm I- 20mm M- M8
Type	Male to Male	Male to Male
Compression Load	40kg	18kg
Compression Deflection	5mm	6mm
Shearing Load	7kg	3.5kg
Shearing Deflection	5mm	-
Thread Size	M8	M8
Material	Natural rubber	Natural Rubber
Metalwork	Steel	Zinc Plate Steel
Diameter	57mm	25mm
Overall Height	84mm	70mm
Maximum Operating Temperature	+70°C	-

In the course of this experiment, there are two types of vibration isolator to be used. The vibration isolator function is to block the motor vibration transmissions from transfer to the frame structure. The vibration isolator will be installed between electric motor and frame as shown in Figure 3.6. Vibration isolator A and B was shown as Figure 3.8 and Figure 3.9. Vibration isolator specifications are shown in Table 3.1.



Figure 3.10 Electric Motor

**Table 3.2:** The specification of electric motor

<b>Brand</b>	Elecktra
<b>Type</b>	3 Phase Induction Motor
<b>Model</b>	AS1359IEC60034/60072BS4999
<b>Frame</b>	1A80M1-2
<b>Power</b>	0.75kW
<b>RPM/rads<sup>-1</sup></b>	2840/47.33
<b>Voltage</b>	4.15V
<b>Frequency (Hz)</b>	50Hz
<b>Mass</b>	13kg
<b>Current</b>	1.6A

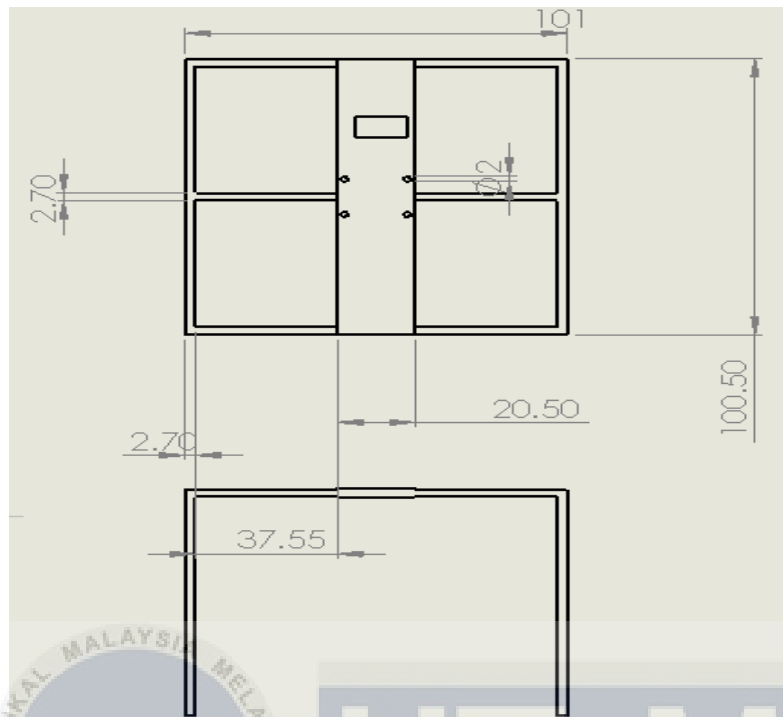


Figure 3.11 Frame and dimension (Top and Side View)

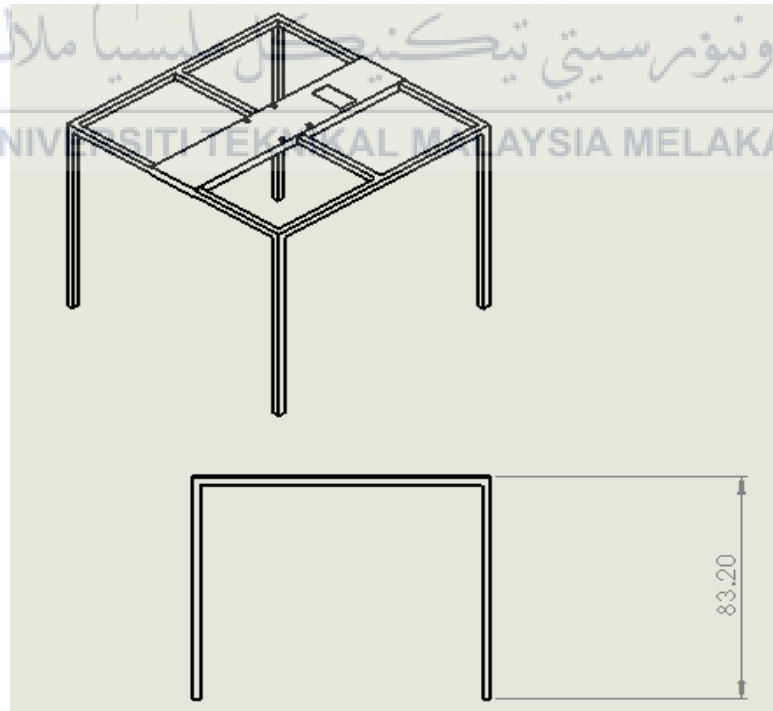


Figure 3.12 Frame and dimension

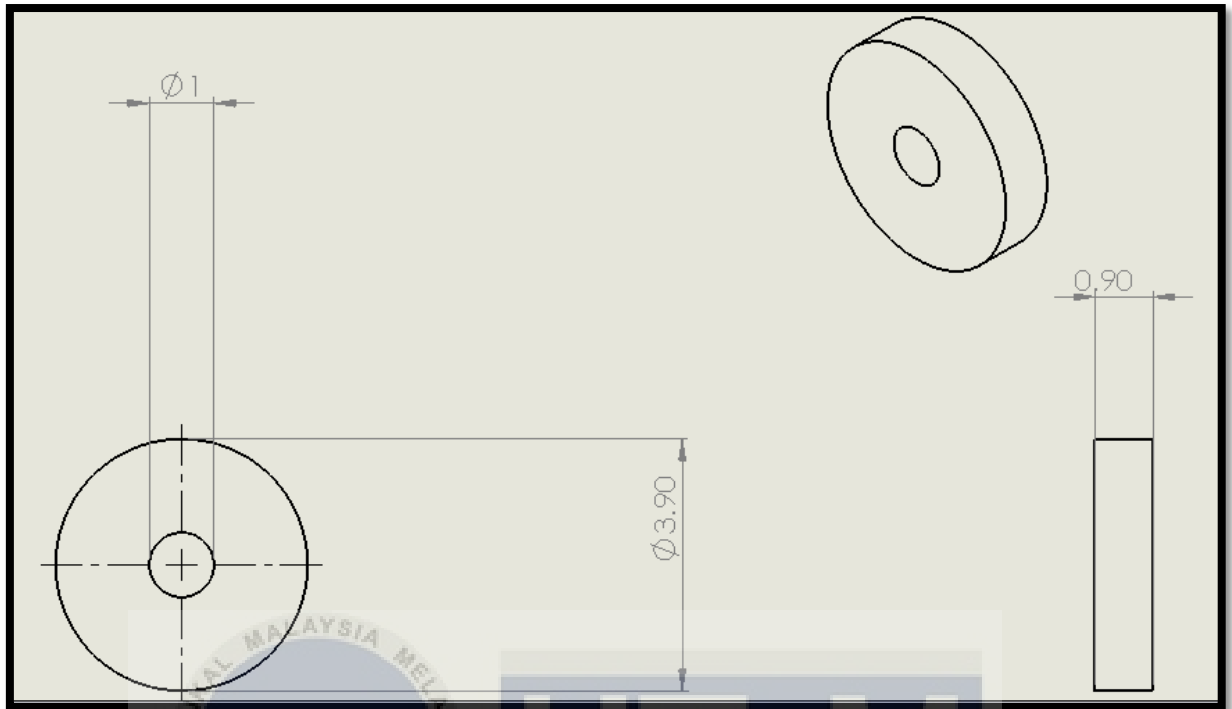


Figure 3.13 Slotted mass and dimension

Figure 3.6 shows the setup and the label for the experiment to be carried out. A motor will be placed at the middle of the frame. The motor image is shown as Figure 3.11 and the motor specifications are shown in Table 3.2. A rotor is located in front of the electric motor. The aim is to produce unbalance rotation when the motor rotates. Figure 3.12 and Figure 3.13 shows the design and the dimension of the frame. The material of the frame is stainless steel. Figure 3.14 shows the slotted mass with dimension.



### 3.4 Measurement of the Performance of Vibration Isolator

Accelerometer sensor is used to measure the vibration frequency. There are four numbers of accelerometer sensors that will be used in the course of this experiment. Each accelerometer sensor is labelled as Sensor 1, Sensor 2, Sensor 3 and Sensor 4. Sensor 1 sensor will be placed vertically on the electric motor. Sensor 1 is placed vertically because to get the vertical vibration signal that experienced by the motor. Sensor 2 will be placed horizontally on the electric motor as shown in Figure 3.5. Sensor 2 will get the reading of the lateral vibration signal when the electric motor rotates. Both Sensor 1 and Sensor 2 acted as the sensor for output vibration. Both sensors are used to receive vibration transmitted signal generated by the electric motor. As the result, the data that's collected from the sensor can be used to find the vibration at of the electric motor. Sensor 3 and Sensor 4 will be placed on the frame as shown as Figure 3.5. Sensor 3 will be placed on the frame in a vertical position while the Sensor 4 will be placed horizontally. Sensor 3 will receive the vertical vibration signals of the frame while Sensor 4 will receive the lateral vibration signals to the frame. Sensor 3 and Sensor 4 act as the input vibration sensors. As the result, all data that were collected will be used to get the transmissibility of the system.

$$T = \frac{\text{Vibration of the frame (output)}}{\text{Vibration of the motor(input)}} \quad (3.4)$$

Table 3.3: Matrix of the experiment

Condition	Without Vibration Isolator	Vibration Isolator	
		A	B
Motor only	✓	X	X
Motor and Rotor only	✓	X	X
Motor, Rotor and Unbalance Mass	✓	✓	✓

Table 3.3 shows the matrix of the experiment that will be conducted. The experiment will start with baseline measurements. The system will be measured by rotating the motor without the presence of any unbalance mass. Thus, no vibration isolator will be attached. Experiments will also conduct with different motor speed. The motor will be operated from speed of 1 Hz to 30 Hz. The speed controller will be used to control the rotation speed. Then, the system will be measured by the presence of the rotor. The motor will start to rotate with the presence of the rotor only. The data will be taken. The speed ranges still the same with the first experiment. The purpose of installing the rotor is to create an unbalance rotation for the electric motor. Next, the system will be measured by the presence of the rotor and slotted mass. The weight of the rotor, screws, slotted mass and rotor stopper will be measured to collect the mass data. The system will be measured without installation of vibration isolator. The experiment will be repeated with the installation different vibration isolator and different rotating speed as shown in Table 3.3.

As the result, the aim of the experiment is to evaluate the performance of the different type vibration isolator. From this experiment, the transmissibility can be measured by using Eq (3.4). Other than that, the resonance of the electric motor will be identified. The comparison can be made between the baseline and the presence of different types of vibration isolator. Last but not least, the performance of each vibration isolator can be compared.

### 3.5 Operating Deflection Shape (ODS) Setup

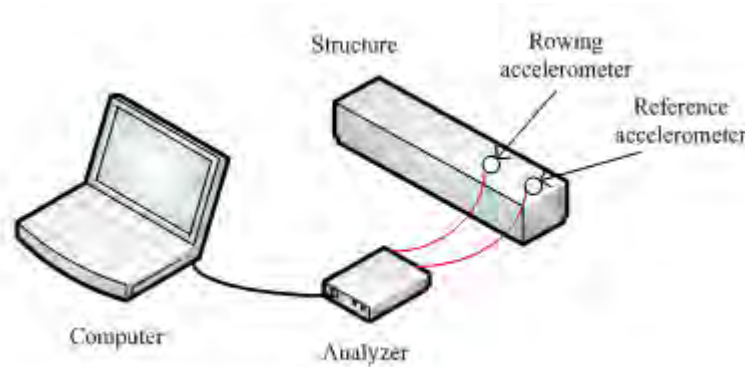


Figure 3.14 General experimental setup for ODS

Table 3.4: Equipment used for ODS measurement.

Instrument	Model	Manufacturer
Accelerometer	Model 3225FI, Dytran ultra miniature teardrop accelerometer	DYTRAN INSTRUMENT, INC
Analyser	Data Physics analyser	Brüel & Kjær Sound & Vibration Measurement

The purpose of the experiment that has to be conducted is to obtain the model of the table frame ODS. Figure 3.15 shows the general experimental setup of the ODS and Table 3.4 shows the equipment used for this experiment. The purpose of the experiment is to obtain all the models of the frame ODS. Initially, the dimension of the frame was measured to decide the number of points to be located for measurement. The model is then created in VMI Vibshape software depending on the number of points in the measurement. Number of points can be added if the model created is unable to show a clear visualization of the frame. In this case the number of points has been decided. There are ninety points that were labelled at the frame and the motor. In this case there are lots of points will be marked on the table frame. The important to properly mark up and label all the points is to

avoid confusion while taking measurements at fixed logical based on the right sequences. It also prevents the points from missed out during the measurement. The dimension of the table frame was measured to decide the number of points to be located for the measurement. The ODS model was created in the VibShape software based on the number of points taken in the measurement

The accelerometer was connected with the analysing and computer to obtain data input for ODS. An accelerometer is attached to a fixed point on the frame to be measured and act as a reference point. The accelerometer was attached to the top corner on the right side of the frame as the reference point. Another accelerometer (rowing) was moved to the remaining points. In order to stimulate ODS of the frame, two types of data are required which are magnitude and phase difference of each point relative to the reference point. The magnitude is taken from the ratio of the transmissibility. In the experiments, accelerometers will take the magnitude and phase of the vibration waves. All the magnitude and phase data that taken from the experiment will interpret in Vibshape Software and it will produce the ODS result for each experiment that have been conducted. The comparison will be made between each vibration isolator when speed at the resonance. When the electric motor approaches the natural frequency it will vibrate hardly. The mode shape will show that the structure moving strongly. When the vibration isolator was installed, the ODS will show different patterns of structural movement. From that, the best vibration isolator will be identified. At same resonance, the vibration isolator with less number of transmissibility can be identified.

## RESULTS AND DISCUSSIONS

### 4.1 Introduction

This chapter will discuss the findings in the study of characterizing the different type of vibration isolators. The system will be tested with three conditions, namely the existence of the motor only, the existing motor and the rotor only and the existence of the motor, rotor and unbalance mass. These three conditions are tested under the state of presence and absence of vibration isolator. After the experimental work is done, the studies continue with the Operating Deflection Shape (ODS) analysis. Operating Deflection Shape (ODS) usually used to analyse the vibration of a structure. ODS analysis method is also used to describe the vibration pattern of a structure that is influenced by a certain vibration source.

### 4.2 Transmissibility

Initially, the project was initiated by running the experiment for the transmissibility of each different system conditions, as shown in Table 4.1.

Table 4.1 Matrix of experiment

Condition	Without Vibration Isolator	Vibration Isolator	
		A	B
Motor only	✓	X	X
Motor and Rotor only	✓	X	X
Motor, Rotor and Unbalance Mass	✓	✓	✓

Figure 4.1 shows the transmissibility against speed for the motor only. The experiment was conducted for two and half hours until the fundamental frequency achieved 30 Hz.

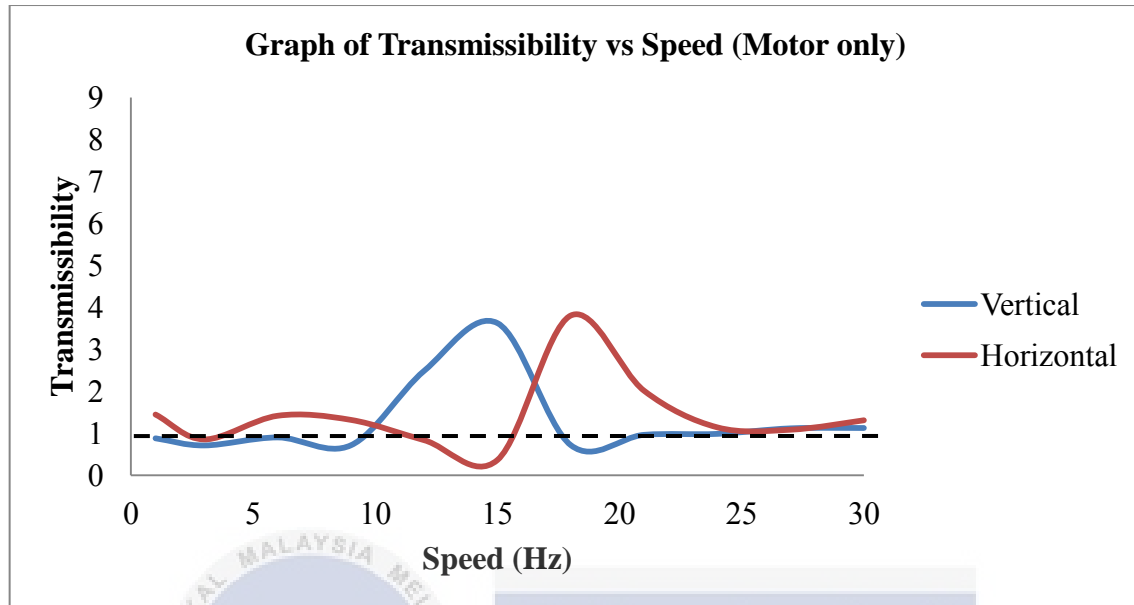


Figure 4.1 Transmissibility against speed for motor only

Based on the Figure 4.1, it shows that the resonance peak appeared at a frequency of 15 Hz in the vertical direction. Whereby, in the horizontal direction, the resonance peak appeared at 18 Hz. Resonance happened when the motor drives the frame structure to oscillate with larger amplitude at these two frequency points. Besides that, the value of transmissibility at vertical direction is equal to 3.627 g at 15 Hz whereby for horizontal direction the transmissibility, T value is 3.8073g at 18Hz. This phenomena happened is due to forcing frequency ( $f_f$ ) and natural frequency ( $f_n$ ) of this system are equal and the T value is greater than 1 ( $T > 1$ ). Moreover, the transmissibility value depends on the stiffness of the system. When, the T is increased, the stiffness at the output energy which is the frame will increase too, but decreases as the input energy (motor). This can be proved by the equation of T as shown below:

$$T = \frac{\text{Output}, Y}{\text{Input}, X} \quad (4.1)$$

where  $Y$  is the output from the frame and  $X$  is the input from the motor. According to Frequency Response Functions (FRF) graph, the horizontal peak is shifted to the right from the vertical peak whereby it indicates the mass controlled by the system.

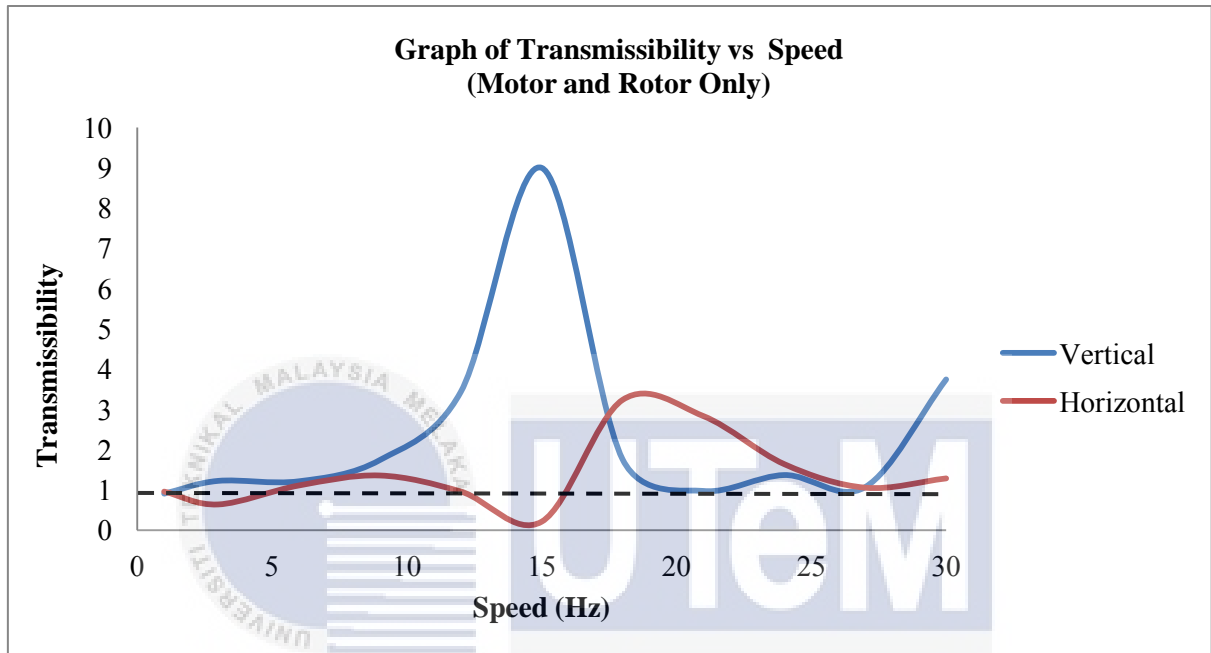


Figure 4.2 Transmissibility against speed for motor and rotor only

As illustrated in Figure 4.2, the resonance peak is higher at vertical direction compared to horizontal direction. The unbalance is usually shown by the high reading of the horizontal or vertical direction. For the vertical direction the resonance peak occurred at 15 Hz whereby its  $T$  value is equal to 9.0 g which is higher than the vertical direction on the Figure 4.1. For the horizontal direction the resonance peak arose at 18 Hz whereby its transmissibility,  $T$  value is equal to 3.236 g. Compared to the motor only condition, the  $T$  value is higher than the motor and rotor only because the rotor acts as additional mass to the system. According to the damping factor,  $\xi$  formula:

$$\xi = \frac{c}{2\sqrt{km}}$$

4.2

where  $c$  is damping ratio,  $k$  is the stiffness and  $m$  is the mass of the system. When the mass increases, the damping factor will decrease. Therefore the damping factor is influenced by the mass of the rotor which leads  $T$  value to increase. This can be proven by equation as followed:

$$T = \frac{1}{2\xi k} \quad 4.3$$

where  $\xi$  is the damping factor and  $k$  is the stiffness.

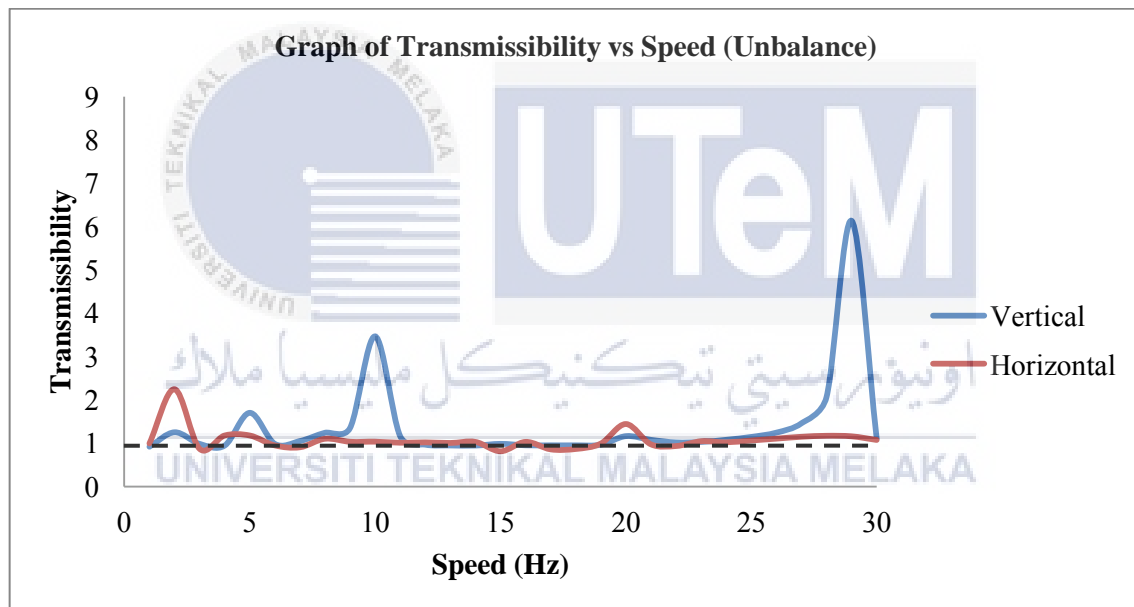


Figure 4.3 Transmissibility against speed for motor, rotor and unbalance load

Figure 4.3 shows that, resonance peak appeared a frequency of 10 Hz for vertical direction and the transmissibility,  $T$  value is 3.468 g. However, horizontal direction the resonance happened at 2 Hz and the transmissibility,  $T$  value is equal to 2.245 g. This finding revealed that the resonance is high at vertical direction than the horizontal direction. Indirectly, the vibratory rate at vertical direction is higher than horizontal direction. The result shows that vertical direction resonance peak and horizontal direction



resonance peak is shifted to the left. Due to that, vertical direction is having first mode and second mode, which means the experimental work show the good agreement with the transmissibility graph, when  $\omega \gg \omega_n$  is known as isolation state.

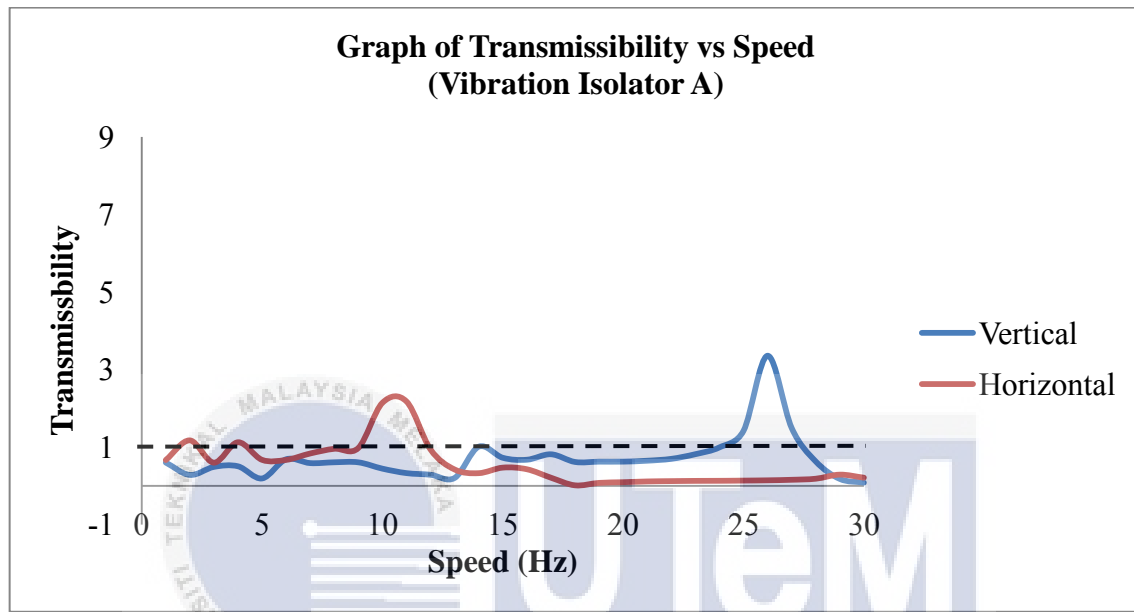


Figure 4.4 Transmissibility against speed for existence of Vibration Isolator A

Figure 4.4 shows the transmissibility against speed for the existence of Vibration Isolator A. At the early stage, the figure shows that there are unwanted peaks appeared from 2 Hz until 4 Hz. This is happening because of the unwanted vibration that comes from the surrounding such as the frame or the base of horizontal direction, the 1<sup>st</sup> peak appeared at the 11 Hz equal to 2.172 g. Compared to the unbalance and the existence of vibration Isolator A the trend in the vertical direction has changed from a peak to no peak opposite to the horizontal direction. This is due to the surface area of the vibration isolator itself. The assumption has been made that the shape of the vibration isolator A is heart shape whereby it block the vibration signal in the vertical direction efficiently. In addition the shape of vibration isolator can only be applied to the system that involves the vertical

vibration signals such as rotating machinery. The suitable frequency range for this vibration isolator A is predicted to be from 0 to 25 Hz.

The experimental result can be verified by using the given formula below:

$$T = \frac{2\xi\omega_n}{\omega} \quad 4.4$$

where  $\xi$  is the damping factor,  $\omega_n$  is the natural frequency and  $\omega$ . Based on the transmissibility graph it is isolation state. Compared to the Figure 4.3 the T value differs from 3.468 g to 0.445 g whereby it is below than 1.

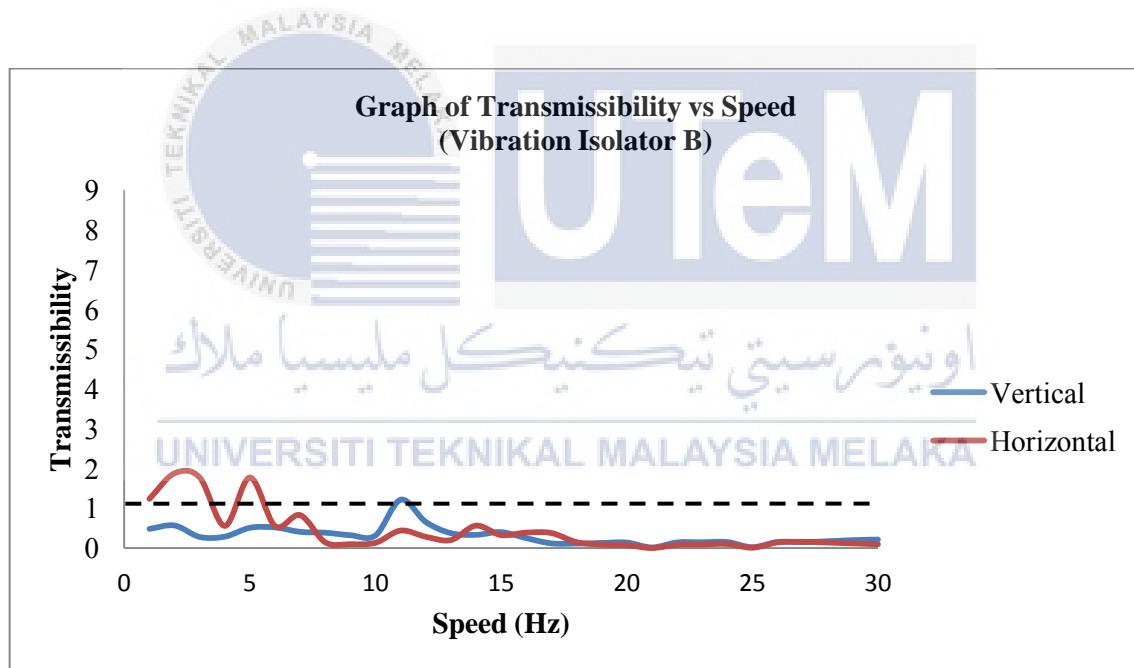


Figure 4.5 Transmissibility against speed for existence of Vibration Isolator B

As illustrated in Figure 4.5 shows that the transmissibility against speed for the existence of Vibration Isolator B. Same to the previous result, there are unwanted peaks at the early stage. This is because the unwanted vibration comes from the surrounding. Compared to the unbalance condition and existence of Vibration Isolator A, Figure 4.5 gives better results with the T value of 0.138 g for both directions a frequency of 10 Hz.

This result indicates that the Vibration Isolator B can isolate better than Vibration Isolator A. It is because Vibration Isolator B can block the vibration signals in both directions. Size of Vibration Isolator A is bigger than Vibration Isolator B. Suppose that the bigger size of vibration isolator should isolate vibration signal well. But vice-versa, Vibration Isolator B can isolate the vibration signal better than Vibration Isolator A. This is because Vibration Isolator B has symmetrical shape.

### 4.3 Operating Deflection Shape (ODS)

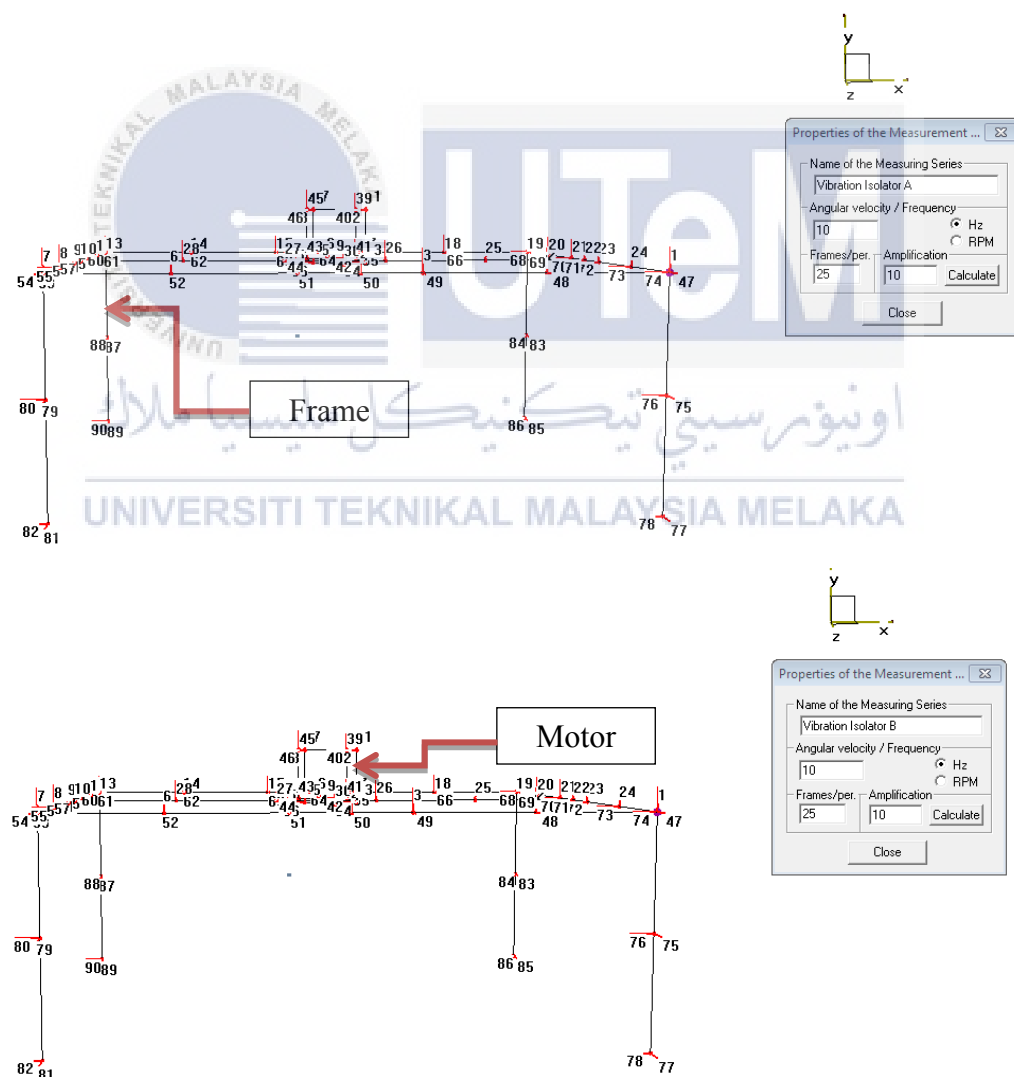


Figure 4.6 Properties of the measurement for Vibration Isolator A and B

Operating Deflection Shape (ODS) is one of the ways on how to look at the movement of the vibration a structure when it is vibrated. When a structure/system is vibrated, the vibration can only be perceived by the senses of touch and cannot be seen with the naked eye. Thus, this ODS was held to examine the ability of two types of vibration isolators which is Vibration Isolator A and B. Thus, the ODS was held to examine the ability of two types of vibration isolators Vibration Isolator A and B. A total of ninety points has been labelled as a location to place the sensors during data acquisition. Figure 4.6 shows the properties of the measurement for Vibration Isolator A and B. Both vibration isolators are tested with a speed of 10 Hz. According to Figure 4.3, the resonance occurred at 10 Hz. Thus, both vibration isolators' performances can be compared based on the images that acquired. ODS images were taken through three types of views, namely front view, side view and top view. Each view is taken by the two types of animation which is a maximum positive animation and a maximum negative animation. A cuboid in the system represents the motor while the structure is in the form of a table representing the frame.

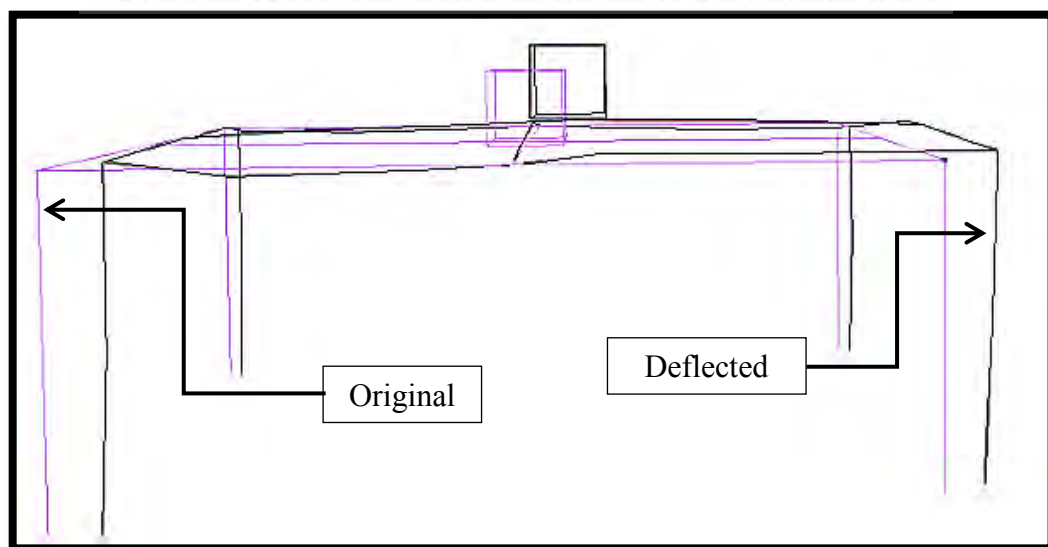


Figure 4.7 Front view maximum positive animation images for Vibration Isolator A

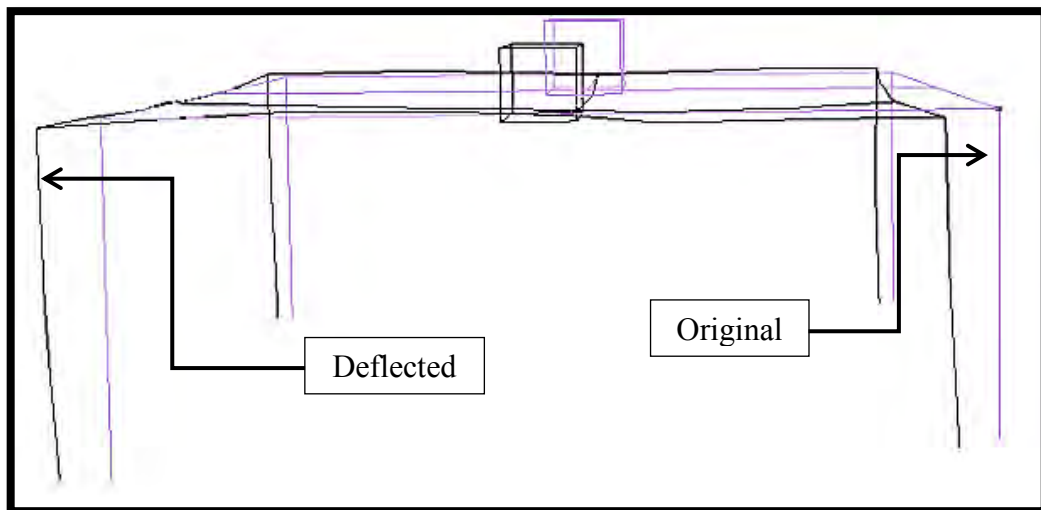


Figure 4.8 Front view maximum negative animation images for Vibration Isolator A

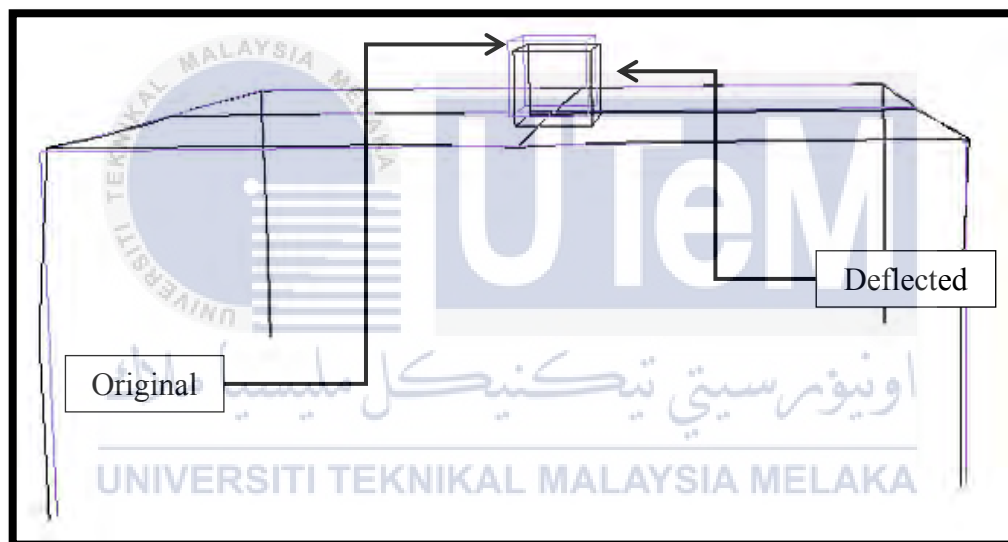


Figure 4.9 Front view maximum positive animation images for Vibration Isolator B

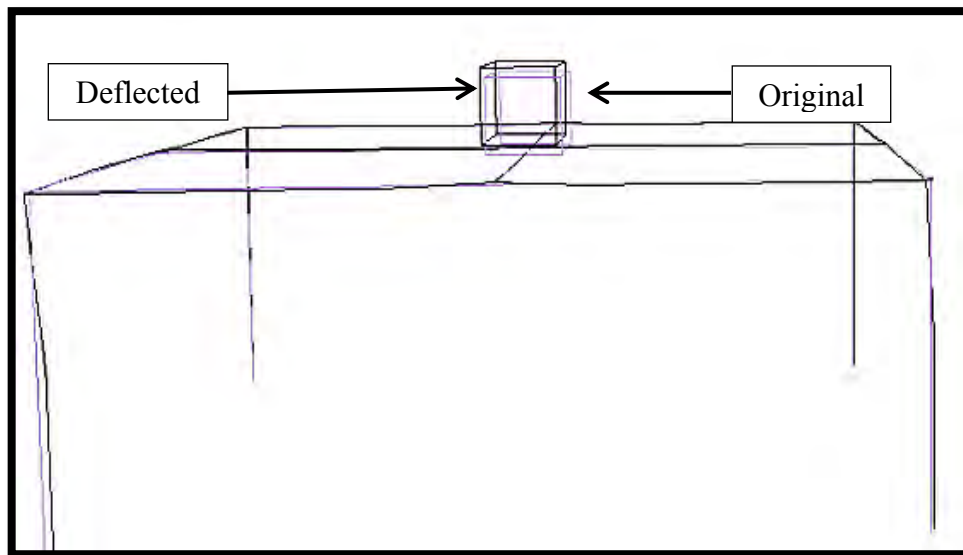


Figure 4.10 Front view maximum negative animation images for Vibration Isolator B

First, a comparison is made against the two types of vibration isolators from the front view of the system. Before the comparison is made, the black line shows that the system is deflected and purple line shows that the system is in rest condition. Figure 4.7 and Figure 4.8 show that the motor moves upward-right and downward-left. Meanwhile, the frame moves to the right at maximum positive animation and to the left at maximum negative animation. Figure 4.9 and Figure 4.10 show that the motor moves upward-left and downward-right. Meanwhile, the frame move right and left respectively. According to the Figure 4.4 and Figure 4.5 the transmissibility value for Vibration Isolator A is higher than the Vibration Isolator B at 10 Hz. The comparison of the transmissibility value for both vibration isolator can relate with the ODS images. The ODS images show that the phase difference for Vibration Isolator A is higher than Vibration Isolator B. The images illustrated that Vibration Isolator A moves vigorously than Vibration Isolator B. From the front view, it shows that Vibration Isolator B can block more vibration signal at vertical direction compared to Vibration Isolator A.

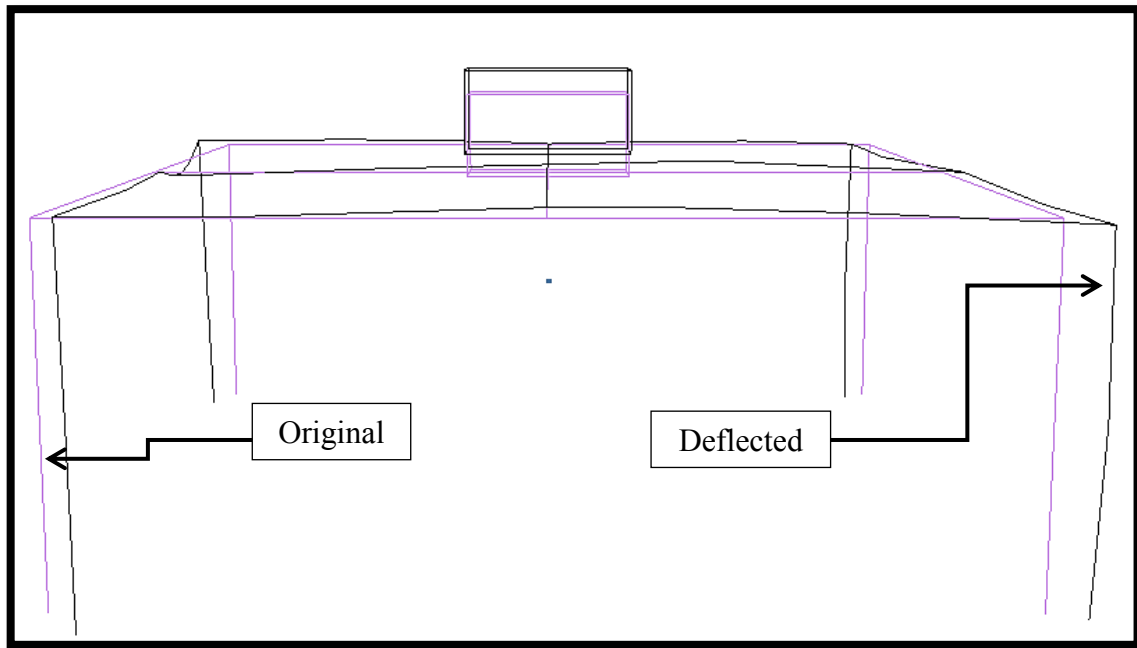


Figure 4.11 Side view maximum positive animation images for Vibration Isolator A

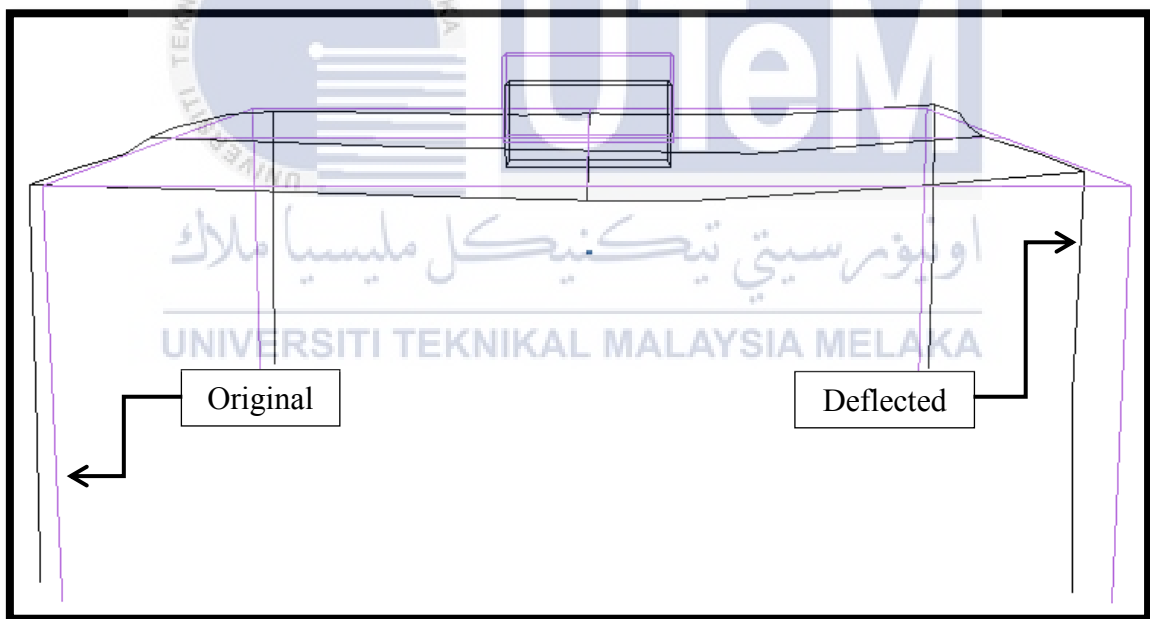


Figure 4.12 Side view maximum negative animation images for Vibration Isolator A

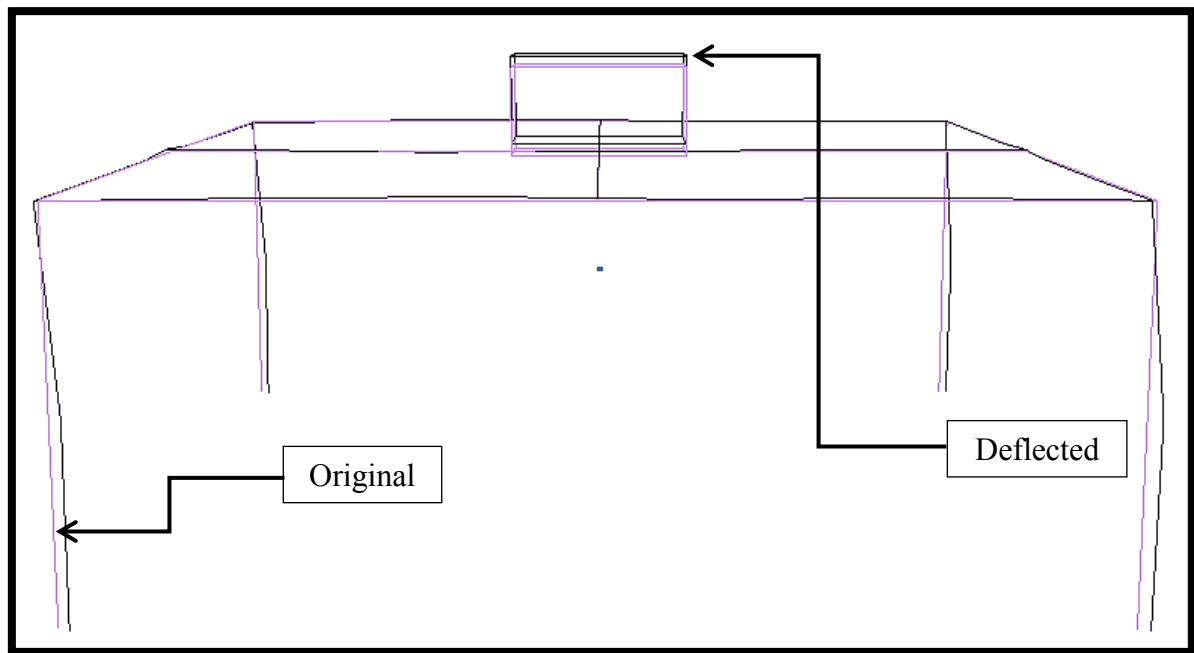


Figure 4.13 Side view maximum positive animation images for Vibration Isolator B

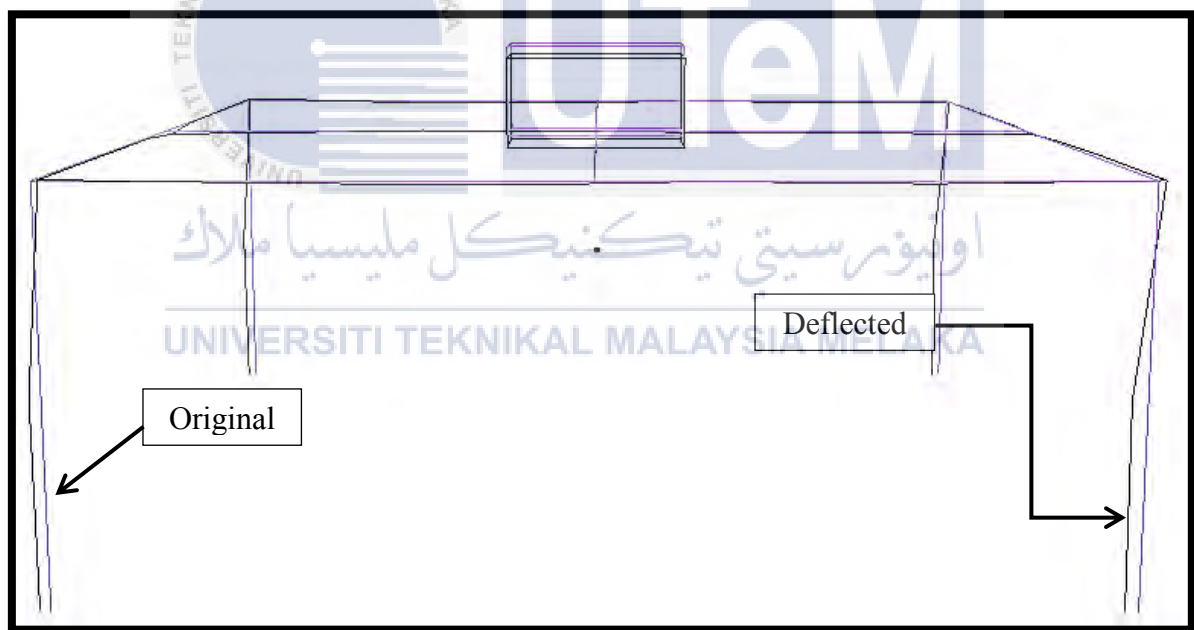


Figure 4.14 Side view maximum negative animation images for Vibration Isolator B

Next, the comparison is made from the side view for the both systems. Figure 4.11 and Figure 4.12 show that the motor pull out the frame and push-down the frame respectively while the motor rotating. The images also show the system moves vigorously because the black line is far away from the purple lines. Different as Vibration Isolator B,



the black line is not far away from the purple line. It means that, Vibration Isolator B 's system less vigorous while the motor rotating. Figure, 4.11 and Figure 4.12 illustrated that when apply Vibration Isolator A it will pull and push the middle of the frame. While the motor was operated, maybe the frame has high elasticity and it could encourage the amplification of the vibration signals. In addition, the properties of the Vibration Isolator A which is heart shaped also contributed the amplification of the vibration signals. Refer to Figure 3.8 and Table 3.1 the vibration isolator A has high compression load/bendable which is less elastic compared to the Vibration Isolator B. Different as Figure 4.13 and Figure 4.14, there is less compression occurred in the middle of the frame. But, obviously the leg of the system was bent and it shows that there is a high compression from the top to bottom.



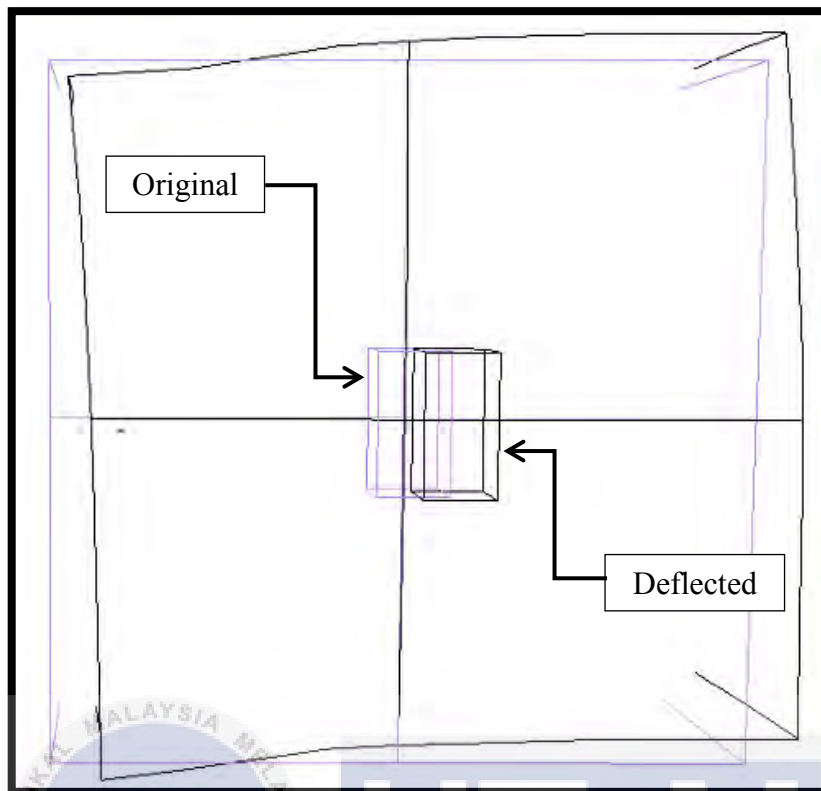


Figure 4.15 Top view maximum positive animation images for Vibration Isolator A

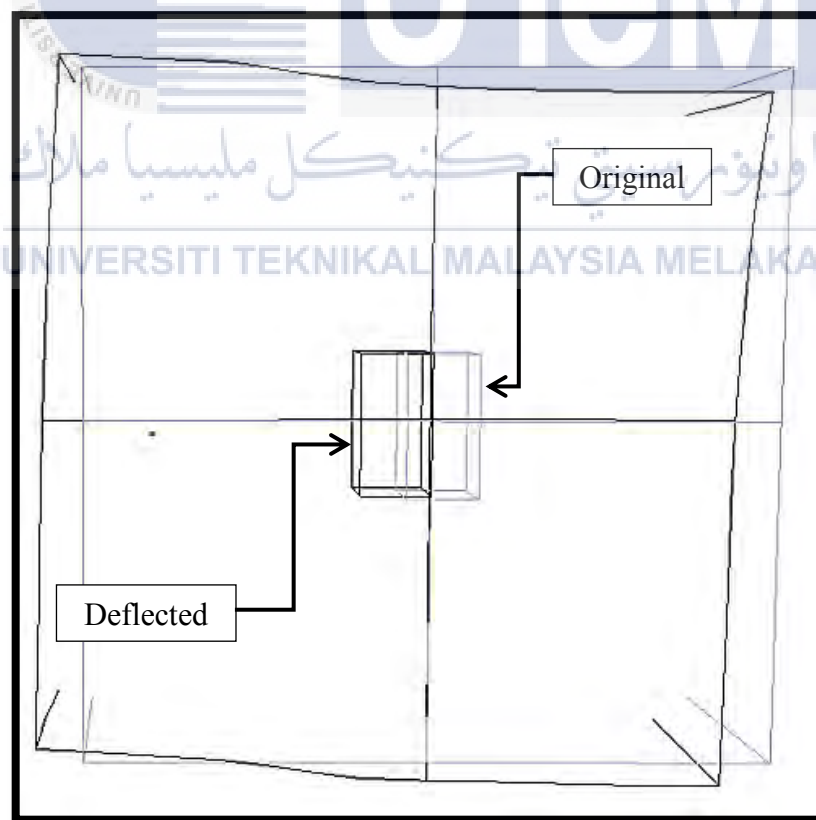


Figure 4.16 Top view maximum negative animation images for Vibration Isolator A

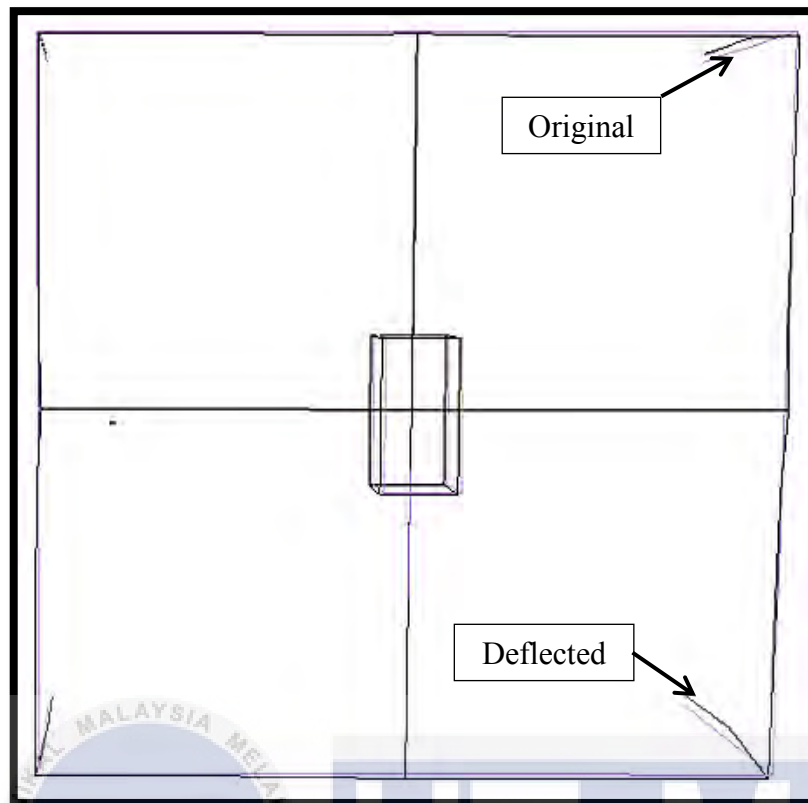


Figure 4.17 Top view maximum positive animation images for Vibration Isolator B

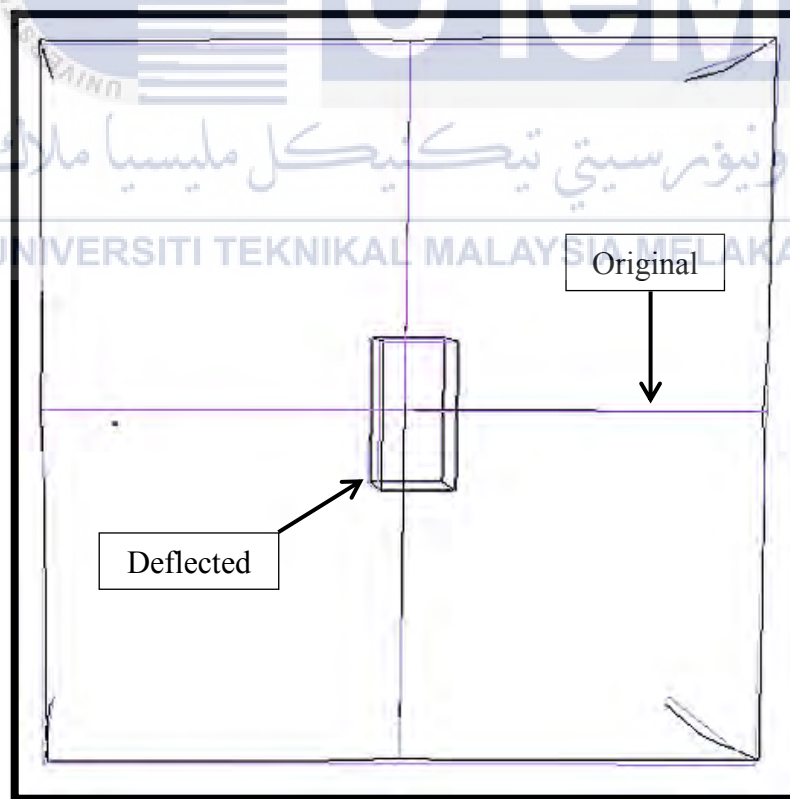


Figure 4.18 Top view maximum negative animation images for Vibration Isolator B

Figure 4.15 and Figure 4.16 it show that the system moves vigorously from the top view. When the motor rotates to the right, it also brings the frame to the right and when the motor rotates to the left, the frame will move to the left too. Obviously, the system moves far away from the original place. Compared to Figure 4.17 and Figure 4.18, Vibration Isolator B gives good isolation because the images show the black line have slide different with the original place/purple line. According to Figure 4.5, the T value is below than 1 g for both directions. The images show the system is less movement. It images relates the data that obtained from the graph. From both graph and ODS data, it shows that Vibration Isolator B is good at blocking the vibration signals that produced by the rotating motor with unbalance mass.



## CHAPTER 5

### CONCLUSION AND RECOMMENDATIONS

As mentioned in the introduction, the purpose of this project is to study what is the characteristic of vibration isolator based on the fundamental study in mechanical vibration course. Second, the aim of this study is to investigate the performance of two types vibration isolators by obtaining the transmissibility,  $T$  value of the system. Third, visualized and compared the effect of vibration isolators when it is applied to the system by ODS method.

This objective has been achieved through the obtaining the characteristic of vibration isolator by conducting analytical studies. Besides, the experimental work was conducted in order to identify the performance of two types of vibration isolators when it is applied in a rotating machine with unbalance mass. Obtain the motor vibration ODS (Operating Deflection State) pattern and visualize the effect of two types of vibration isolator by using VibShape Software.

From the study of the vibration isolation of a rotating motor, it is found that the vibration isolator can isolate the transmission of the vibration signals that produce from the rotating machine to the platform/frame. Other than that, the performance of each vibration isolators can be determined by conducting the experiment to identify the highest transmissibility,  $T$  value at certain operating speed. Besides, the characteristic of each vibration isolator also can be determined by using ODS. ODS can be used to visualize either the vibration isolator isolate at one direction or multi-directions. Thus, the

transmissibility,  $T$  and the ODS data that had been obtained can be compared. As the result, Vibration Isolator B performs better than Vibration Isolator A.

At the early stage of the project, an analytical study had been conducted in order to gain knowledge regarding the fundamental of mechanical vibration especially in vibration isolation course. After that, two types of vibration isolator were chosen. The assumption had been made based on the vibration blocking direction characteristic. Vibration Isolator A has a heart shape according to Figure 3.8. Thus, Figure 3.9 shows that Vibration Isolator B has a cylinder shape. In an assumption, maybe Vibration Isolator A can tackle vibration transmission in one direction which is horizontal direction only. Meanwhile, Vibration Isolator B can tackle more vibration transmission from multi directions.

In order to test the performance of the vibration isolator, each of the vibration isolator had been installed between a rotating machine and the frame. An unbalance mass was attached at the rotor of the motor. The function of the unbalance mass is to create a vibration. The motor was operated at several speeds from a speed of 1 Hz to 30 Hz. There are five different conditions that had been tested based on Table 4.1. As the result, Figure 4.1 until Figure 4.5 shows that Vibration Isolator B can isolate the vibration signal better than Vibration Isolator A. Other than that, both types of vibration isolator are good at isolating vibration from the horizontal direction.

To strengthen the studied conducted, ODS of the system had been obtained. The ODS was compared at 10 Hz speed. Based on Figure 3.4, resonant occurred at 10 Hz. So that, the data of both vibration isolators were taken at 10 Hz rotating speed. The movement/deflection of the system when the different vibration isolator applied had been compared as shown as Figure 4.7 until Figure 4.18. The images show that Vibration

Isolator A moves vigorously than Vibration Isolator B. Vibration Isolator B moves less vigorously either in vertical direction and lateral direction.

The research limited in several ways. There is a few suggestion to improve the research in the future. First, the data that had been obtained is less significant. This is due to the error during conducting the experiment. Based on Figure 4.4 and Figure 4.5, there are unwanted signal appeared at frequency speed of 1 Hz to 5 Hz. This is due to the unwanted vibration signal from the surrounding. In fact, the frame legs were not well isolated. The signal cannot be identified whether the signal is resonance. For example, other vibration source that transmitted to the system. An improvement should be done for future study by installing the vibration isolators at the frame's legs

Second, the limitation during conducted this project is the lack of information about the specification of the vibration isolator in the research of stiffness and damping factor of vibration insulator material, shear stress, compression value, deflection, shape of the vibration isolator. The experiment cannot be compared mathematically. In future, the study about the properties of the material should be conducted. So that, the result can be compared between experimental, theoretical and solid mechanical properties of the vibration isolator.

Third, in the future suggestion the vibration isolator can be changed to the new model. So that, the performance of different type of vibration isolator can be studied. Thus, the characteristic for the new type vibration isolator can be determined.

Other than that, the speed of the motor and mass of the unbalance mass can be increased So that, the vibration isolator can be tested to identify the maximum performance of the vibration isolator.

The finding indicates that there are need to isolate the vibration waves that are produced from the defect machine. This project also is one of the ways that help us to study the performance of the vibration isolator in multi-direction. Vibration Isolator widely used in industrial to isolate the defected machine. This is useful for the condition monitoring course. The vibration signal can harm the machine and other machine near it if the vibration signals are not well isolated. Other than that, the project helps us to know the characteristic of the vibration isolator in the different types of the blocking direction.





## REFERENCES

- Bae, W., Kyong, Y., Dayon, J., Park, K., & Wang, S., (2011). Scaling the operating deflection shapes obtained from scanning laser Doppler vibrometer. *Journal of Nondestructive Evaluation*, vol. 30, no. 2, pp. 91-98.
- Carella, A., Brennan, M. J., Waters, T. P., & Shin, K., (2008). On the design of a high-static—low- dynamic stiffness isolator using linear mechanical springs and magnets. *Journal of Sound and Vibration*. doi:10.1016
- Carrella, A., Friswell, M.I., Zotov, A., Ewins, D.J., & Tichonov, A., (2009). Using nonlinear springs to reduce the whirling of a rotating shaft. *Journal of Mechanical Systems and Signal Processing*.
- Coppola, G. (2010). On the Control Methodologies of a Novel Active Vibration Isolator. Lakehead University, Thunder Bay, Canada.
- Jing, X.J., Lang, S.A., & Billings, S.A., (2011). Non-linear influence in the frequency domain: alternating series. *Systems and Control Letters*, 60 (11) 295–309.
- Kramer, C., (2001). Comparison of ambient and forced vibration testing of civil engineering structures. Retrieved from: [www.vibetech.com](http://www.vibetech.com)
- Lacoste, L., (1934). A new type long period vertical seismograph, *Physics*.
- Lamancusa, J.S., (2002). Vibration isolation. *Noise and Vibration Control Engineering*, 42(23) 429-450

Levent, M. E., & Sanliturk, K. Y., (2003). Characterisation of vibration isolators using vibration test data. Tenth International Congress on Sound and Vibration, Stockholm, Turkey.

Lynch, J.P., Wang, Y., Loh, K. J., Yi, J., & Yun, C., (2006). Performance monitoring of the Geumdang Bridge using a dense network of high resolution wireless sensors. *Smart Materials and Structures*, vol. 15, no. 6, pp. 1561-1575,

Milovanovic, Z., Kovacic, I., Brennan, M.J. (2009). On the displacement transmissibility of a base excited viscously damped non-linear vibration isolator. *Journal of Vibration and Acoustics*, 131054502–054507.

Naibiao, Z., & Kefu, L., (2011). Characterization of an electromagnetic vibration isolator. *Journal of Electromagnetic Analysis and Applications*. doi:10.4236/jemaa.2011.312079

Potter, R., & Richardson, M.H., (2003). *Identification of the modal properties of an elastic structure from measured transfer function data 20th international instrumentation symposium*. Albuquerque, New Mexico.

Ravindra Bachan & Mallik Kalai (1994). Performance of non-linear vibration isolators under harmonic excitation. *Journal of Sound and Vibration*, 170 (1994)325–337.

Schwarz, B.J., & Richardson, M. H., (2004). *Introduction to operating deflection shapes*. Jamestown: California.

Weekes, B., & Ewins, D., (2015). Multi-frequency, 3D ODS measurement by continuous scan laser Doppler vibrometry. *Mechanical Systems and Signal Processing*, vol. 58-59, pp. 325- 339.

Yonghui, H., Lu, Y., Lijuan, W., Xiangchen, Q., & Yong, Y., (2016). On-line Continuous Measurement of the Operating Deflection Shape of Power Transmission Belts Through Electrostatic Sensing.

Zhenlong, X., Xingjian, J., & Li, C., (2012). The transmissibility of vibration isolators with cubic nonlinear damping under both force and base excitations. *Journal of Sound and Vibration*, 332(15)1335–1354.

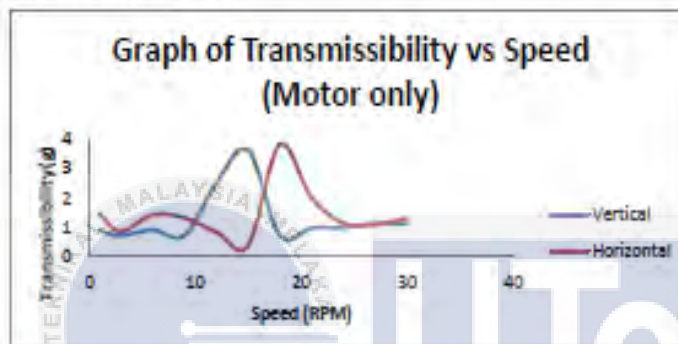


## APPENDIX A

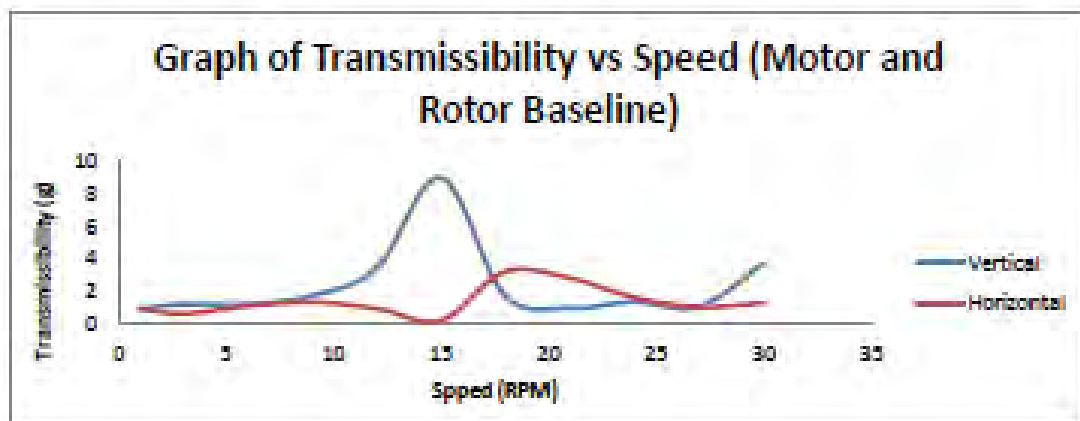
No.	Activities	2016					2017				
		September	October	November	December	January	February	March	April	May	June
1	Title Approval										
2	Title Briefing										
3	Researchers of Background Study										
4	Literature Review										
5	Research of Methodology										
6	Preparation & Submission of Progress Report										
7	Measurement Vibration Isolator Performance										
8	Operating Deflection Shape (ODS)										
11	Data Collection										
12	Data Analysis										
13	Preparation & Report Submission										
14	Preparation of Seminar										

## APPENDIX B

RPM	Vertical	Horizontal
1	0.880747	1.446119
3	0.710642	0.832417
6	0.901884	1.416338
9	0.71449	1.318071
12	2.490884	0.833679
15	3.626813	0.362517
18	0.717795	3.80728
21	0.963479	2.013892
24	0.986449	1.139678
27	1.117921	1.083531
30	1.126124	1.30891



RPM	Vertical	Horizontal
1	0.905248	0.9582
3	1.222352	0.638613
6	1.212627	1.110448
9	1.740689	1.35814
12	3.431722	0.960296
15	8.997961	0.210576
18	1.75858	3.236176
21	0.972645	2.833208
24	1.367318	1.639208
27	1.069055	1.054693
30	3.742302	1.285453

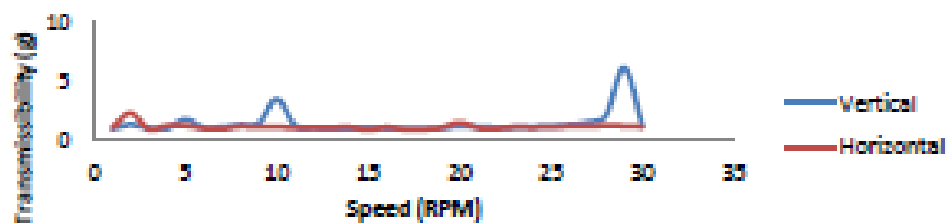


RPM	Vertical	Horizontal
1	0.920433	0.996808
2	1.253879	2.245109
3	0.985929	0.874164
4	0.946739	1.180043
5	1.703144	1.180043
6	0.985973	0.952187
7	1.050618	0.908933
8	1.242722	1.104987
9	1.352704	1.035724
10	3.468481	1.037686
11	1.161911	1.013762
12	0.967564	1.022889
13	0.949357	1.008332
14	0.946739	1.032164
15	0.986593	0.816843
16	0.95285	1.033671
17	0.952705	0.861366
18	0.95232	0.869896
19	0.965639	0.994491
20	1.164594	1.444025
21	1.078451	0.976064
22	1.019937	0.937963
23	1.029662	1.046949
24	1.079498	1.023598
25	1.146089	1.065148
26	1.245445	1.107943
27	1.461492	1.150996
28	2.06851	1.173564
29	6.136685	1.161349
30	1.106453	1.077217

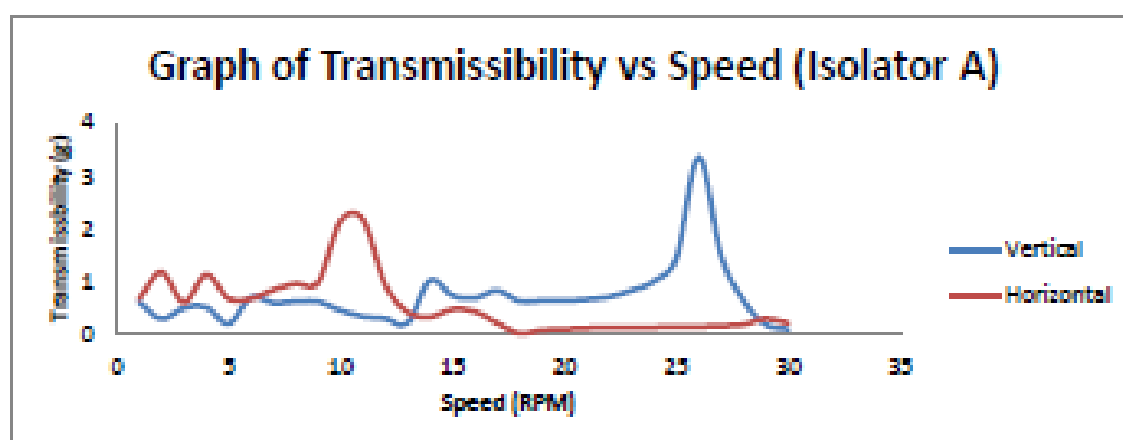
UTeM

UNIVERSITI TEKNIKAL MALAYSIA MELAKA

Graph of Transmissibility vs Speed  
(Unbalance)



RPM	Vertical	Horizontal
1	0.602439	0.660238
2	0.282413	1.167036
3	0.490063	0.392696
4	0.303813	1.119392
5	0.191835	0.664712
6	0.686443	0.663683
7	0.587377	0.829017
8	0.609118	0.930307
9	0.607799	0.971122
10	0.444649	2.136733
11	0.329672	2.171816
12	0.287733	0.931111
13	0.203227	0.413343
14	1.011937	0.321182
15	0.723062	0.464377
16	0.674198	0.422623
17	0.814976	0.20442
18	0.617426	0.007578
19	0.624702	0.070697
20	0.625342	0.087586
21	0.649296	0.107783
22	0.697722	0.116034
23	0.817939	0.122523
24	0.993342	0.124149
25	1.420863	0.129847
26	3.337291	0.136627
27	1.492937	0.130392
28	0.630027	0.177838
29	0.179446	0.283044
30	0.083184	0.204847

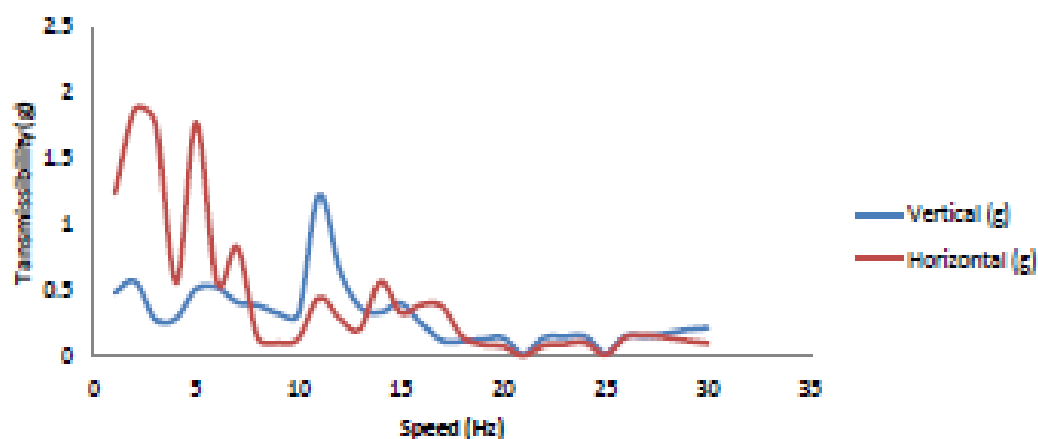


Speed (Hz) Vertical (g) Horizontal (g)

1	0.487394	1.241017
2	0.571807	1.882271
3	0.283943	1.77749
4	0.291991	0.561372
5	0.514701	1.77749
6	0.523704	0.55742
7	0.412505	0.832213
8	0.391031	0.149484
9	0.327743	0.104327
10	0.322929	0.13876
11	1.220663	0.443063
12	0.661408	0.289666
13	0.378671	0.206132
14	0.336756	0.568293
15	0.404723	0.331938
16	0.254364	0.394162
17	0.12186	0.383183
18	0.117538	0.155018
19	0.13274	0.09185
20	0.143966	0.079362
21	0.020379	0.00703
22	0.145647	0.087644
23	0.150373	0.095535
24	0.155406	0.107762
25	0.025715	0.015856
26	0.155665	0.147427
27	0.153826	0.162666
28	0.175644	0.144511
29	0.20355	0.122165
30	0.219071	0.101145

UTeM

Tansmissibility vs Speed (Vibration Isolator B)





## APPENDIX C

